Pharmacological Ablation of Astroglia in a Rat Model of Parkinson's Disease

By

Chase Groulx

A thesis to the Faculty of Graduate and Post-Doctoral Affairs in partial fulfillment of the requirements for the degree of:

Master of Science

In

Neuroscience

Carleton University

Ottawa, Ontario

Abstract

Parkinson's disease is an age-related neurodegenerative motor disorder that currently has no effective treatment to halt the degeneration. While most studies examining this disease have focused on the neurons of the basal ganglia, there is now increasing interest in what role the astrocytes play in the pathogenesis and progression of the disease. Using a well-documented model of parkinsonian symptoms, 6-hydroxydopamine, as well as an astrocyte-specific gliotoxin, D-alpha-aminoadipic acid, we examined how dopamine cells in the substantia nigra would react to the sudden loss of the surrounding astrocytes. We compared the effects of the neurotoxin against the effects of the gliotoxin using a variety of behavioural measures as well as immunohistochemical analysis. We found that a modest loss of astrocytes in the substantia nigra leads to dopaminergic cell death that is comparable to that which is seen in the group that received 6-hydroxydopamine. Furthermore, we observed behavioural deficits in the rats that received the gliotoxin to be on par with rats that received the neurotoxin. Together, the data suggests that a slight loss of astrocytes in the substantia nigra has detrimental effects on neuronal survival and motor behaviour, demonstrating that the pathology observed in Parkinson's disease could stem from astrocytes. Future studies will examine possible causes for astrocytic death or dysfunction in Parkinson's disease.

Acknowledgements

I would like to thank Natalina, Stephanie, Jess Chris and the entire Salmaso Lab for their help and support throughout this entire project. Without all of them, there wouldn't be anything to write about. This project was definitely hard at times, and I'm glad I had the support of a great lab to make it through.

I would also like to thank my committee members for taking the time to read and review my work. I'm grateful to have people in my community that are willing to share their knowledge and experience with me.

Nikki, thank you for helping me through this entire process, from day one to now. I'm sure it hasn't been easy at times, and I appreciate all that you have done to help.

TABLE OF CONTENTS

List of Figures

Introduction

Parkinson's Disease

Parkinson's disease (PD) is an age-related neurodegenerative disease that was first characterized by James Parkinson in 1817 (Parkinson, 2002). First dubbed "the shaking palsy", he described a disease that had a very slow onset of a tremor in one limb that gradually and consistently worsened, and as it progressed, other motor symptoms could be observed (Parkinson, 2002). Today, these are known as the four cardinal symptoms of PD; tremor at rest, gait and balance disturbances, muscular rigidity and a slow initiation of voluntary movements known as bradykinesia (Sveinbjornsdottir, 2016). The unilateral onset of symptoms in the early-stages, progressing to the contralateral side with increasing severity is also considered a hallmark of the disease today (Sveinbjornsdottir, 2016). It would not be until 1919, when Konstantin Tretiakoff published a doctoral dissertation that we would have any understanding of the pathology of this disease. In the dissertation, Tretiakoff described severe neuronal cell loss specifically in the substantia nigra pars compacta (SNc) along with inclusion bodies of patients who had died with PD (Lees et al., 2008).

The substantia nigra was first described in 1786 (Haber, 2014), but it was not known until the 1960's that the neurons in this region contained dopamine (DA) (Ehringer and Hornykiewicz, 1960; Bazelon et al., 1967). Many studies have highlighted that DA cells in the SNc appear to be particularly vulnerable to degeneration (Hirsch et al., 1988a; Blesa et al., 2015; Surmeier et al., 2017; Surmeier, 2018), but the cell may not actually be what causes the motor symptoms associated with PD. DA neurons contain the enzyme tyrosine hydroxylase (TH), the rate-limiting

enzyme in DA production (Daubner et al., 2011). It has been shown that TH^+ immunoreactivity in the SNc decreases quite rapidly after a diagnoses of PD, however, the total number of DA neurons decreases at a slower pace (Kordower et al., 2013), suggesting that the DA neurons may have a loss of function prior to the actual degeneration of the cell. Interestingly, the presentation of the cardinal symptoms of PD has been estimated to occur when there is only around a 30% loss of the nigro-striatal system, continuing to fall to about 60-80% has been lost at the time of death (Cheng et al., 2010).

While the specific dopaminergic cell loss is an important and well-known feature of PD, it is the secondary finding of Tretiakoff, the inclusion bodies that are co-localized with the cell death, that has really become a feature of interest for understanding the pathology. These inclusions were named Lewy bodies, after Friedrich Lewy, who discovered similar inclusions in the vagus nerve (Engelhardt and Gomes, 2017). When Lewy discovered these inclusions in 1912, they were known to be associated with PD, but they were not understood very well until the 1960's. In 1965, electron microscopy of autopsy tissue from PD patients lead to the discovery that Lewy bodies were comprised of abnormal filaments (Duffy and Tennyson, 1965). It was not until the end of the 20th century that immunoelectron microscopy identified the main constituent of Lewy bodies to be α-synuclein (α-SYN). The researchers concluded that the α-SYN found in Lewy bodies was unassembled, and suggested that the presence of the α-SYN filaments may contribute to the neuronal cell death seen in PD (Spillantini et al., 1998)

Pathology of Parkinson's Disease

PD has a very well-described and predictable pattern of expression, that describes the neuropathology all the way from the prodromal phase to the end-stage, known as Braak staging. Primarily, this staging follows the propagation of Lewy bodies from inception, describing where the disease starts, as well as how and when the motor symptoms arise (Braak et al., 2003). In the first stage, the Lewy bodies seen in PD develop first in the dorsal motor nucleus of the vagal nerve, the intermediate reticular zone, and the olfactory bulb. While Lewy bodies are observed in many areas in this stage, it is mainly the Lewy bodies in the vagal nerve that propagate into other areas of the brain normally associated with PD (Braak et al., 2004). Stage 2 involves the Lewy bodies starting to be seen in the raphe nuclei, and then in stage 3 the Lewy bodies start to invade the midbrain regions, specifically affecting the SNc (Braak et al., 2003). Once the Lewy bodies reach the temporal mesocortex in stage 4, a sufficient amount of neurodegeneration has occurred in the SNc for the cardinal symptoms of PD to present. It is in this stage that a diagnoses of PD would typically be made (Braak et al., 2003, 2004). Finally, in stages 5 and 6, Lewy bodies are able to be found in the prefrontal cortex and high-order sensory association areas. In these late stages, the dopaminergic neurons in the SNc are almost completely wiped out, corresponding with a complete presentation of the cardinal symptoms of PD(Braak et al., 2004). At this point, Lewy bodies can be seen in almost all areas of the brain and significant cell death is seen in many parts, leading to the late stage symptoms seen in PD such as dementia (Irwin et al., 2012).

Astrocytes and Their Functions

Around the mid 1850's, Rudolph Virchow noticed previously unknown structures that filled the space between neurons and seemed to hold them together. He gave these structures the name *nervenkitt*, meaning 'nerve glue', and the translation is now what we collectively call the

structures today, ‘neuroglia’ (Landhuis, 2018). The main constituent of neuroglia and the most abundant cell type in the brain, are specialized glial cells known as astrocytes. These cells were named for the star-like appearance by Michael von Lenhossek in 1893 (Fan and Agrid, 2018). In 1909, Ramon y Cajal categorized astrocytes into two main types that are still used today, *protoplasmic* astrocytes, and *fibrous* astrocytes. *Protoplasmic* astrocytes are found in the gray matter, and have several large processes extending from the body with many fine processes extending from the large processes. This leads to *protoplasmic* astrocytes having a large spherical-like distribution, with there being very little overlap between astrocytic projections from neighbouring astrocytes. *Fibrous* astrocytes on the other hand, are found in the white matter of the brain and are named as such because they have many long fibrous processes extending from the cell body, appearing to be less dense than *protoplasmic* astrocytes (Sofroniew and Vinters, 2010; Zhang and Barres, 2010). This classification of astrocytes is based solely on their morphological differences, and both carry out a wide range of essential and complex functions within the central nervous system (CNS).

The wide range of functions that astrocytes carry out starts very early on, as astroglial cells (astrocytes as well as their precursors, radial glia) generate neurons during embryonic development, and to a much lesser extent in the adult brain (Vaccarino et al., 2007). Astrocytes also help guide neurites during development by creating boundaries with extracellular matrix molecules that promote the axon’s growth towards their target (Powell and Geller, 1999). Synaptogenesis in the developing CNS is also controlled by astrocytes, with immature astrocytes secreting proteins that permits the development of synapses during a specific critical period of development (Christopherson et al., 2005). Furthermore, astrocytes are critical for the maturation and stabilization of functional synapses late in development (Ullian et al., 2001). Astrocytes are

so important for neuronal development, that in culture, neurons developing without contact to astrocytes, fail to form synapses at all, further emphasizing the importance of cell-to-astroglia contact in the developing CNS (Hama et al., 2004).

Neurons are not the only cell that astrocytes make direct contact with, as many astrocytic endfeet surround cerebral blood vessels. Together with specialized endothelial and mural cells that make up the blood vessels in the CNS, the astrocytic endfeet help comprise the blood-brain barrier (BBB). This barrier carefully controls which molecules, ions and proteins can make it into the CNS environment, regulating CNS homeostasis with much greater control than is found anywhere else in the body (Daneman and Prat, 2015). This specialization of the cerebrovasculature, appears to be controlled by astrocytes through the secretion of src-suppressed C-kinase substrate (SSeCKS), modulating the endothelial cells to have the specialized properties and increasing tight junction formation (Lee et al., 2003). Furthermore, it has been shown that non-neuronal endothelial cells can be induced to have properties indicative of CNS endothelial cells in the presence of astrocytes (Janzer and Raff, 1987), providing more evidence that astrocytes tightly regulate and maintain the properties of the BBB.

Astrocytes serve as the intermediary between cerebral blood vessels and neurons, and as such, they closely regulate cerebral blood flow (CBF) (Zonta et al., 2003). CBF is controlled such that the blood flow increases with synaptic activity, and decreases in the absence of it, in a process known as neurovascular coupling (NVC) (Mishra, 2017). It was long thought that astrocytes mediate NVC through Ca^{2+} and K^{+} signalling to hyperpolarize and relax the smooth muscle tissue in response to a release in glutamate from increased synaptic activity (Attwell et al., 2010), however new evidence has shown that this might not be the case. Using optogenetic stimulation of astrocytes paired with pharmacological manipulations, it was demonstrated that astrocytes

mediate vasodilation in response to synaptic activity mainly through the release of K^+ from their endfeet onto the blood vessels. It was found that the blockade of K^+ signalling had a very large effect on CBF, whereas blocking Ca^{2+} signalling had no effect on CBF(Masamoto et al., 2015). Taken together, the evidence suggests that astrocytes are critical for the normal function of cerebrovasculature, contributing to neuronal homeostasis.

In addition to regulating CBF, astrocytes also help regulate the fluid homeostasis of the CNS through the coupling of aquaporin-4 (AQP4) with inward rectifying K^+ channels (Nagelhus et al., 2004). These two channels are heavily expressed on astrocytic endfeet that contact blood vessels (Zador et al., 2009), leading to activity-dependant changes in fluid volume that helps regulate the solute concentrations of the extracellular fluid (Nagelhus et al., 2004). Astrocytes also tightly regulate extracellular glutamate concentrations, removing it using a sodium-potassium mediated transporter (Sattler and Rothstein, 2006). The expression of these transporters appears to be highly plastic, responding rapidly to changes in synaptic activity, rather than extracellular concentrations of glutamate (Armbruster et al., 2016). This quick response means that over 90% of the glutamate released in the brain is transported into astrocytes and recycled, allowing neighbouring synapses to fire independently of each other (Marcaggi et al., 2003). The function of astrocytes in maintaining homeostasis of the CNS environment is critical for healthy neuronal function, however there is now evidence that suggests astrocytes play an even more direct role in synaptic function.

Astrocytes have been shown to be able to discriminate between the activation of different axonal pathways, integrate that information (Perea and Araque, 2005), as well as release gliotransmitters such as glutamate, D-serine and γ-aminobutyric acid (GABA). Together, this evidence suggests that astrocytes are involved with active information processing within the CNS

(Halassa et al., 2007). It has been shown that by attenuating gliotransmission, cortical slow oscillations are reduced, suggesting that astrocytes are critical for functional axonal communication (Fellin et al., 2009). The modulation of neuronal activity by astrocytes has given rise to the term 'tripartite synapse', which alludes to the exchange of information between the pre- and post-synaptic neuron as well as with astrocytes within the axonal network (Halassa et al., 2007; Perea et al., 2009). Astrocytes have also been shown to modulate the strength of a synapse through many different mechanisms (Stellwagen and Malenka, 2006; Schwarz et al., 2017), with a growing body of evidence that supports the notion of astrocytes as the main drivers of synaptic plasticity (Barres, 2008; De Pittà et al., 2016; Dvorzhak et al., 2018).

Astrocytes and Neuroprotection

Astrocytes respond to any CNS insult by rapidly changing their gene expression and even their morphology to deal with the insult, a reaction that is known as astrogliosis. This response is not an all-or-nothing reaction to an insult, but rather a carefully controlled set of mechanisms that is in line with the severity and specific to the type of insult (Sofroniew, 2009). Due to this spectrum in response, there have been many factors that are implicated in triggering astrogliosis, including but not limited to; cytokines, glutamate, noradrenalin, and reactive oxygen species (ROS) (John et al., 2003; Swanson et al., 2004; Bekar et al., 2008). Even more diverse, is the number of possible changes to gene expression that occur in the reactive astrocytes in response to the insult, affecting almost every aspect of known astrocytic function. Despite the vast amount of possibilities, an upregulation in glial fibrillary acidic protein (GFAP) gene expression has been found to be a key feature of astrogliosis, occurring in all levels of the astrogliosis response (Sofroniew, 2009).

GFAP is the main cytoskeletal protein found in astrocytes, and its upregulation during astrogliosis leads to hypertrophy of the astrocyte, which is generally thought to help protect the nervous system during acute stress (Hol and Pekny, 2015). When the insult to the CNS is severe, astrocytes start to rapidly divide (Colodner et al., 2005), and when combined with the GFAP upregulation, the astrocyte's swelled processes overlap to create a dense structure known as a glial scar (Sofroniew and Vinters, 2010). This glial scar serves various protective functions such as directly protecting neurons from further damage, limiting the spread of inflammatory cells, and normalizing the CNS environment (Shih et al., 2003; Faulkner et al., 2004; Voskuhl et al., 2009; Anderson et al., 2016; Freitas-Andrade and Naus, 2016). While there is a wealth of evidence supporting the neuroprotective qualities of reactive astrocytes, there is also evidence that suggests they inhibit the regeneration of neurons, as well as have neurotoxic qualities (McKeon et al., 1991; Bradbury et al., 2002; Fitch and Silver, 2008; Alilain et al., 2011).

According to new and emerging evidence, reactive astrocytes have the ability to be either neuroprotective or neurotoxic during astrogliosis, exhibiting polar gene expression profiles in response to different types of insults (Zamanian et al., 2012). A study by Zamanian *et al.,* discovered that astrogliosis caused by ischemia induces a molecular phenotype that would suggest the reactive astrocytes are neuroprotective, but lipopolysaccharide (LPS)-induced reactive astrocytes express genes that suggestive of a neurotoxic phenotype (Zamanian et al., 2012). This discovery led to the classification of reactive astrocytes as either being an A1 or an A2 subtype based on what genes are upregulated. When astrocytes become reactive and exhibit the A1 phenotype, they lose many homeostatic functions that are attributed to healthy astrocytes, and instead secrete a toxin that signals for apoptosis in nearby neurons and oligodendrocytes (Liddelow et al., 2017). A1 astrocytes appear to be induced by the release of fragmented mitochondria by

microglia (Joshi et al., 2019) as well as microglial secretion of interleukin 1α (IL-1 α), tumour necrosis factor (TNF-α) and complement component 1, subcomponent q (C1q) (Clarke et al., 2018). Reactive astrocytes with the A2 phenotype are reliably induced by ischemia, and exhibit an upregulation in neurotrophic factors, promoting neurite growth and synapse formation after injury (Liddelow et al., 2017; Su et al., 2019). The induction mechanism for A2 astrocytes is much less understood, though high levels of Prokineticin-2 (Neal et al., 2018) as well as a decrease in microRNA-21 (Su et al., 2019) have both been postulated as possible mechanisms.

Astrocytes and Parkinson's Disease

The role of astrocytes in PD was not an extensively researched topic until recently, as it was considered a disease of neuronal dysfunction, along with many other neurodegenerative disorders. The focus has now shifted onto the role of astrocytes in neurodegenerative disease pathogenesis (Liddelow and Sofroniew, 2019), as it has become increasingly clear that they are no longer passive support cells (Barres, 2008; Allen and Barres, 2009; Sofroniew and Vinters, 2010; Landhuis, 2018). This new focus has led to many new discoveries about both astrocytes as well as PD, with some being intuitive, and others very surprising.

One of the more surprising findings is that many aspects of astrocytic function are in part, controlled by genes that have a causative role in the development of PD (Booth et al., 2017). In many cases, the dysfunction of these genes has been shown to lead to a break-down in normal astrocytic function, causing them to be detrimental to the survival of surrounding neurons (Solano et al., 2008; Choi et al., 2018). These changes have typically been thought to be in response to the neurodegeneration as part of the astrogliosis response, but recent evidence suggests that it may be

the other way around. It has been demonstrated that transgenic α-SYN expression specifically in the astrocytes of mice was sufficient to induce an inflammatory response in the midbrain that was also accompanied by DA cell loss (Gu et al., 2010), lending support to the idea that astrocytic dysfunction may actually be a symptom of PD that leads to severe DA cell loss, rather than a response to DA cell loss. It should be noted that this study used a model that expressed α-SYN in all astrocytes throughout the brain, making it unclear whether the effects were due to astrocytic dysfunction within the SNc alone. When specifically looking at the genes that have been associated with PD, the notion of astrocytes as the main target of PD starts to gain steam.

DJ-1 (also known as PARK7) is implicated in the pathogenesis of PD, as a mutation in it leads to early-onset PD (Bonifati et al., 2003). DJ-1 is normally abundantly expressed in astrocytes (Bandopadhyay et al., 2004) appearing to mediate astrocytic neuroprotection and neuronal repair in response to many types of insults (Mullett et al., 2013; Choi et al., 2018; De Miranda et al., 2018). In PD cases however, the protein becomes aggregated within reactive astrocytes (Rizzu et al., 2004), signifying the proteins loss of function.DJ-1 knock-out (KO) models show that its absence impairs astrocytic pro-inflammatory mediation (Ashley et al., 2016), astrocytic glutamate uptake (Kim et al., 2016), and astrocytic mitochondrial function (Larsen et al., 2011). The impairment in astrocytic mitochondrial function is especially important because the deletion of DJ-1 also appears to cause a dysfunction in the scavenging of mitochondrial H_2O_2 (Andres-Mateos et al., 2007), suggesting a large increase in oxidative damage as a result of its dysfunction. Further adding to this, leucine-rich repeat kinase 2 (LRRK2), a gene found to be mutated in a relatively large amount of both idiopathic and familial PD cases (Gilks et al., 2005; Nichols et al., 2005), has been shown to reduce PINK1/parkin dependant mitophagy (Bonello et al., 2019). In sum, genes associated with PD appear to directly cause impairments in astrocytic function, that in part, leads

to neurodegeneration. However, these results do not seem to explain why only some areas of the brain are susceptible.

Since astrocytes are one of the most abundant cell types within the brain, referring to them as a homogenous cell type is a bit of an oversimplification. Astrocytes in one region of the brain may be vastly different from astrocytes in a neighbouring region, varying in aspects such as morphology, gene expression and response to insult (Zhang and Barres, 2010; Khakh and Sofroniew, 2015). It has been shown in culture that midbrain astrocytes react differently to a 6-hydroxydopamine (6-OHDA) insult than hind- or forebrain astrocytes. The midbrain astrocytes protected DA neurons by secreting larger amounts of brain derived neurotrophic factor (BNDF) than astrocytes from the other regions (Datta et al., 2018). When examining subregions within the mid brain, it appears that SNc astrocytes are unable to protect DA neurons from a neurotoxin, whereas ventral tegmental area (VTA) astrocytes are able to (Kostuk et al., 2019). This finding is especially interesting, given that DA neurons in the VTA of humans with PD appear to be relatively undamaged compared to DA neurons in the SNc (Hirsch et al., 1988b). While research has typically tried to find specific vulnerabilities in midbrain DA neurons to explain their susceptibility to degeneration in PD (Giguère et al., 2019), these findings would suggest that it is actually the specific astrocytes' inability to protect the DA neurons that leads to the neuropathology of PD.

Adding to this, α-SYN, a core feature of PD pathology, has several interesting interactions with astrocytes. The uptake of aggregated α-Syn has been shown to occur in astrocytes, though interestingly, it appears to occur only after a certain level of α-SYN aggregation has occurred in local neurons (Kovacs et al., 2014). Research has also shown that astrocytes readily take up aggregated from the surrounding neurons and area quite efficiently, but does not transfer it back

to neurons in as efficient of a manner (Loria et al., 2017). Taken together, the data would suggest that astrocytes are responding to the accumulation of the dysfunctional proteins by trying to clear them from the surrounding neurons. This rapid uptake of α-SYN begins to stress the astrocytes, leading to mitochondrial damage (Rostami et al., 2017). As a defensive mechanism, the stressed astrocytes send out tunneling nanotubes and actively transfer the aggregated α-SYN to healthy astrocytes elsewhere via lysosomal trafficking (Abounit et al., 2016; Rostami et al., 2017). This transfer is possible mediated by toll-like receptor 2 (TLR2) signalling, as blocking the signalling with an inhibitory antibody was able to stop the transfer of α-SYN between astrocytes as well as neurons, leading to a decrease in the pro-inflammatory response (Kim et al., 2018). The implication of these findings is that the astrocytes appear to initially be providing protection to their surrounding neurons by helping to clear the filaments. However, when the amount of aggregated α-SYN increases, this protective mechanism goes awry and ends up harming the astrocytes, which in turn may lead to them negatively affecting the neurons.

Interestingly, aggregated α-SYN appears to also cause glutamate excitotoxicity by enhancing glutamate release from astrocytes through a mechanism independent of the glutamate transporter (Sarafian et al., 2017). Under normal conditions, the mere presence of astrocytes dramatically reduces the amount of neuronal death due to excitotoxicity (Zhang et al., 2019), as they rapidly uptake and recycle the nearby glutamate (Marcaggi et al., 2003; Sattler and Rothstein, 2006). However, the brains of PD patients have been shown to have lower levels of dynamin-like protein 1 (DLP1) in astrocytes, a protein that is involved in mitochondrial fission. The knock down of DLP1in rat cortical astrocytes leads to the impairment of the astrocytes' ability to protect against glutamate excitotoxicity, as well as increasing the intracellular Ca^{2+} response to extracellular levels of glutamate (Hoekstra et al., 2015). There is also evidence that shows α-SYN

aggregation is promoted by calcium (Nath et al., 2011). Together this suggests that there may be a snowball effect of α-SYN enhancing glutamate release from astrocytes, which then leads to increased excitotoxicity and intracellular Ca^{2+}, and as a result, α-SYN aggregation is increased. While this remains to be tested experimentally, the idea highlights just one of the many ways astrocytic function is directly intertwined with PD pathology.

The research conducted to date has vastly expanded our understanding on how astrocytes function under the pathological conditions of PD. While many studies have examined the effects of upregulating or knocking out specific astrocytic genes, few have looked at the total cumulative effect of astrocytes on the pathogenesis of PD. A previous study by another group has shown that astrocytes in the SNc become reactive at around 9 days post- 6-OHDA lesion, around the same time that the number of TH^+ cells begins to drop in the SNc (Stott and Barker, 2014), suggesting that the survival of TH^+ cells is at least in part dependant on the normal functioning of astrocytes. While it could be argued that astrocytes are responsible for PD pathology, previous data from our lab has shown that optogenetic stimulation of astrocytes is protective against a striatal 6-OHDA lesion and ameliorated the associated behavioural symptoms, suggesting an exciting therapeutic role for astrocytes in PD. However, this, like many of the studies that have looked at astrocytes in neurodegeneration, consider astrocytes to be secondary, or reacting to the degeneration. Few studies have considered the possibility that astrocytes may be the primary cause of the neurodegeneration. The goal of the proposed study is therefore, to determine how DA cells react to the sudden loss of astrocytes within the SNc. Using a striatal 6-OHDA partial lesion in combination with an astrocyte-specific gliotoxin, D-alpha aminoadipic acid (D-AAA) injected into the SNc, we will examine the role of astrocytes in the pathogenesis of PD. 6-OHDA is a commonly used model of PD, selectively ablating monoaminergic neurons through mainly oxidative damage.

By injecting this toxin directly into the striatum, we can selectively target DA cells in the SNc, observing behavioural deficits after approximately 14 days (Su et al., 2018). D-AAA is an astrocyte specific gliotoxin that is taken up by astrocytes via the sodium-dependant glutamate transporter (Brown and Kretzschmar, 1998) and exerts its gliotoxic effect through the prolonged inhibition of protein synthesis (Nishimura et al., 2000). The delay in the appearance of behavioural deficits with 6-OHDA alone will allow us to determine if the presence or absence of astrocytes in the SNc accelerates or delays the degeneration of DA cells.

Given the integral role that astrocytes have in neuronal function under non-pathological conditions, we hypothesize that astrocytic loss or dysfunction would be sufficient to trigger neurodegeneration. As such, we also hypothesize that the combination of 6-OHDA and D-AAA will lead to a more rapid and overall greater amount of degeneration within the SNc, as well as the corresponding motor deficits. To test this, we will track the motor behaviour of the rats over several time points and examine the SNc for DA cell death as well as markers of reactive astrocytes. The table below summarizes the hypotheses made.

Table 1: Dopamine cell death hypothesized per treatment condition

Treatment Group	D-AAA	Saline
6-OHDA	++++	++
Saline	++	No Change

- The number of + signs indicate increasing degrees of pathology

Methods

Animals

Both male and female Long-Evans rats were purchased from Charles River (Quebec, Canada) at 250-300g. All animals were pair-housed upon arrival in standard (395mm x 346mm x 213mm, Techniplast) fully transparent polyphenilsulfone cages with basic cage enrichment, including PVC tube, Enviro-dri bedding and *ad libitum* food and water access. Immediately following the surgical procedure, the animals were then singly-housed in standard (395mm x 346mm x 213mm, Techniplast) fully transparent polyphenilsulfone cages with Enviro-dri bedding and *ad libitum* food and water access. The rats were maintained on a 12-hour light/dark cycle in a temperature controlled (21 degrees Celsius) environment with food and water available as desired. All animal use procedures were approved by the Carleton University Committee for Animal Care, according to the guidelines set by the Canadian Council for the Use and Care of Animals in Research. Experimental timeline and animal use are summarized in the table below.

Group	Baseline/Day 0	Surgical Procedure	Day 5	Day 10	Day 20	Sex/Total
Saline/Saline	Rotarod/ Digigait™	SNc- Saline Str- Saline	Rotarod/ Digigait™	Rotarod/ Digigait™	Rotarod/ Digigait™	M-7 F-8 All- 15
Saline/6-OHDA	Rotarod/ Digigait™	SNc- Saline Str- 6-OHDA	Rotarod/ Digigait™	Rotarod/ Digigait™	Rotarod/ Digigait™	M-7 F-8 All-15
D-AAA/Saline	Rotarod/ Digigait™	SNc- D-AAA Str- Saline	Rotarod/ Digigait™	Rotarod/ Digigait™	Rotarod/ Digigait™	M-7 F-8 All-15

D-AAA/6-OHDA	Rotarod/ Digigait™	SNc- D-AAA Str- 6-OHDA	Rotarod/ Digigait™	Rotarod/ Digigait™	Rotarod/ Digigait™	M-7 F-8 All-15

Table 2: Experimental timeline and animal use summary table

Surgery

This experiment combined the striatal 6-OHDA-lesion as has been used previously in our lab in conjunction with a SNc D-AAA lesion similar to Banasr and Duman (Banasr and Duman, 2008). The experimental group underwent stereotaxic surgery to inject both 6-OHDA and D-AAA using isofluorane as a volatile anaesthetic. Slow-release Meloxicam (Chiron, Guelph, Ontario) was administered at 4 mg/kg I.P. immediately prior to surgery. A guide cannula, 360 μm in internal diameter, was aimed at the dorsal striatum (Males; AP: 1.2, ML: 3.0, DV: -5.4, Females; AP: 1.2, ML: 3.0, DV: -5.3) and another at the SNc (Males; AP: -5.8, ML: 2.0, DV: -7.2, Females; AP: -5.8, ML: 2.0, DV: -7.1). D-AAA (100 μg/μL solution) was infused into the SNc at a rate of 0.1 μL/min for 10 minutes (1 μL total volume), with the guide cannula remaining undisturbed for 10 minutes following the infusion. Immediately following that, 2 μL of a 10 μg/μL 6-OHDA solution was infused into the dorsal striatum at a rate of 0.4 μL/min for 5 minutes, with the guide cannula being left in for 1 minute following the infusion procedure. The incisions were then closed with monofilament nylon sutures and Vetbond tissue adhesive. Following the surgical procedure, the animals were provided with hydrogel electrolyte and nutritional supplement for 24 hours to assist with eating and drinking. To control for the 6-OHDA and D-AAA injections, 3 control groups were used. The sham D-AAA lesion control group received an equivalent infusion of saline in the SNc and an infusion of 6-OHDA in the striatum. The sham 6-OHDA lesion control group received

an equivalent infusion of saline in the striatum and an infusion of D-AAA in the SNc. The final sham lesion control group received equivalent infusions of saline in both the striatum and SNc. Animals were monitored immediately following each procedure and again one hour later, followed by twice daily monitoring for 4 days. The animals were observed for general condition, decreased locomotor activity or lethargy, decreased grooming and other unusual behaviours judged consistent with distress.

Rotarod

In order to track the motor deficits that are characteristic of 6-OHDA lesion-induced neurodegeneration, the rotarod was used, as it is a well validated test that provides an overall assessment of balance, coordination and strength. In the apparatus, there is a rotating drum that was continually and gradually increased from 4 to 44 RPM over 300 s and is raised ~1 foot above a foam bottom. Rats that have sufficient SNc neurodegeneration to induce motor impairments will generally be unable to remain on the rotating drum as long as rats that do not have SNc neurodegeneration. During the test days, rats were placed on the drum facing the back of the apparatus, the rotation and timer was then started, and the time to fall off was recorded as the outcome measure. Rats underwent 4 trials each day, separated by 30 minutes to prevent fatigue. The rotarod test was conducted on day 0 (baseline), day 5, day 10, and day 20 of the experiment. The equipment was cleaned with PREvail between trials.

DigiGait™

In order to track gait abnormalities that result from a unilateral 6-OHDA dopaminergic lesion, the DigiGait™ gait analysis system was used. The DigiGait™ system is comprised of a clear motorized treadmill and a high-speed camera which records the ventral surface of the animal for analysis. The analysis software produces many indices of gait for each limb, allowing for comparison between the lesioned and non-lesioned limbs within the subject. During the test days, rats were placed on the treadmill surface and the speed of track was increased from 0 to 21 cm/s. When the track is at 21 cm/s, a ~3 s video of the animal walking uninterrupted was saved. Only 1 video from each animal was taken from each test day and was analyzed using the DigiGait™ analysis software automatically, with artifacts from the gait signals being corrected manually. The DigiGait™ test was conducted on day 0 (baseline), day 5, day 10, and day 20 of the experiment. The equipment was cleaned with 70% ethanol between animals.

Animal Sacrifice and Immunohistochemical Analysis

24 hours following behavioural testing completion, all animals were sacrificed. Animals were injected with 44mg/kg sodium pentobarbital. Upon loss of toe pinch reflex, animals underwent cardiac perfusion. 50 mL of saline was perfused through the left ventricle to flush out blood, followed by 50 mL of 4% paraformaldehyde (4% PFA) to fix the tissue. Brains were then extracted immediately after perfusion and placed into vials containing a solution of 4% PFA and 30% sucrose. The vials were stored at 4 ºC for 72 hours, then drained and transferred to a -80 ºC freezer for storage. Brains were sectioned into 50 sister sections at 30µm thick on a Leica cryostat. The sections were then processed for immunohistochemistry for the analysis of TH^+ cells and GFAP in the SNc. The sections were pre-blocked in Phosphate buffered saline (PBS) containing 0.3% Triton and 10% horse serum, followed by overnight incubation in the primary antibody at

the appropriate concentration (*see Table 3*). After the overnight incubation, the sections were washed thoroughly in PBS and then incubated for 2 hours in a fluorescent secondary antibody of the correct species (*see Table 3*). The processed sections were then imaged on a Carl Zeiss LSM 800 confocal microscope (Carl Zeiss, Toronto, ON) using a 20x plan-apochromat objective and Zen software (Carl Zeiss, Toronto, ON). TH and GFAP immunoreactivity was quantified using ImageJ (imagej.net) to measure fluorescence by selecting the area of interest and dividing total area by the optical density of the fluorescent channel.

Table 3: List of antibodies used for Immunohistochemistry

Antibody	Manufacturer	Species	Dilution
TH (#22941)	Immunostar	Mouse	1:500
GFAP (#134436)	Abcam	Chicken	1:1000
Donkey Anti-Mouse	Invitrogen Fluor 546	N/A	1:500
Donkey Anti-Chicken	Invitrogen Alexa Fluor 488	N/A	1:1000

Statistical Analysis

All data was analyzed using IBM SPSS Statistics Data Editor. The independent variables were neurotoxin, gliotoxin and time. The dependant variables are latency to fall off rotarod, step angle coefficient of variation (CV), ataxia coefficient, number of $GFAP^+$ cells, and number of TH^+ cells. A 2x2x4 repeated measures analysis of variance (ANOVA) was conducted with neurotoxin (6-OHDA vs. Saline), gliotoxin (D-AAA vs. Saline) and time for latency to fall of rotarod, step angle CV, ataxia coefficient. If overall model was significant, then ANOVAs were followed up with two tailed t-test comparisons with a Bonferroni correction for non-orthogonal comparisons. Probability values were considered significant when $p < 0.05$. A 2x2 ANOVA was conducted with neurotoxin (6-OHDA vs. Saline) and gliotoxin (D-AAA vs. Saline) for number of $GFAP^+$ cells and number of TH^+ cells separately. If the overall model was significant, ANOVAs were then

followed up with two tailed t-test comparisons. Probability values were considered significant when $p < 0.05$.

Data Transformations

Significant individual variability between experimental groups was observed in many of the dependant variables at baseline. To account for these differences, the data was transformed into a percentage of baseline score for day 5, day 10, and day 20.

Results

Prior to analyzing our results, we analyzed whether there were any sex differences in any of the measure examined. No statistically significant differences were observed between male and female rats overall on any measures; therefore, males and females were analyzed together.

Behavioural Analyses

Motor Deficits

Rotarod Performance Test. A 2x2x4 repeated measures ANOVA was conducted to assess the effect of a neurotoxin (6-OHDA vs. Saline) and gliotoxin (D-AAA vs. Saline) over time (baseline, day 5, day 10, day 20) on the Rotarod which is a measure of balance, overall coordination, and strength. Latency to fall off the Rotarod was recorded in seconds and expressed as a percentage of baseline performance. The ANOVA revealed a significant interaction of neurotoxin x gliotoxin x time $F_{(3, 48)} = 2.785$, $p = 0.05$ *(Figure 1)*. Post hoc tests revealed a

significant difference on day 20 between Saline/Saline controls and each of the other groups (p <0.01) such that control rats stayed on the rotarod longer than all others *(Figure 1)*. When mice are repeatedly tested on the rotarod, animals are expected to improve their performance over repeated exposures to the task, making the rotarod not only a measure of motor behaviour, but also of motor learning (Shiotsuki et al., 2010). Because we had a significant interaction of time x neurotoxin x gliotoxin, we tested whether motor learning (significant improvement from baseline to Day20) was observed in all groups. Results of a post-hoc one-way ANOVA showed a significant difference in performance over time in the Saline/Saline group $F_{(3, 36)} = 6.203$, $p < 0.05$ as well as the D-AAA/Saline group $F_{(3, 39)} = 3.880$, $p = 0.05$ *(Figure 1),* suggesting that motor learning was observed in these two conditions, but not in either of the 6-OHDA treated groups. Post hoc tests for the Saline/Saline group revealed a significant difference between baseline and all of the other timepoints (day 5, day 10, day 20) (p <0.01). Post hoc tests for the D-AAA/Saline group revealed that the baseline score was significantly different from both day 5 and day 10 (p <0.01), suggesting that this group only learned until Day 10, after which presumably the effects of the lesion decreased performance.

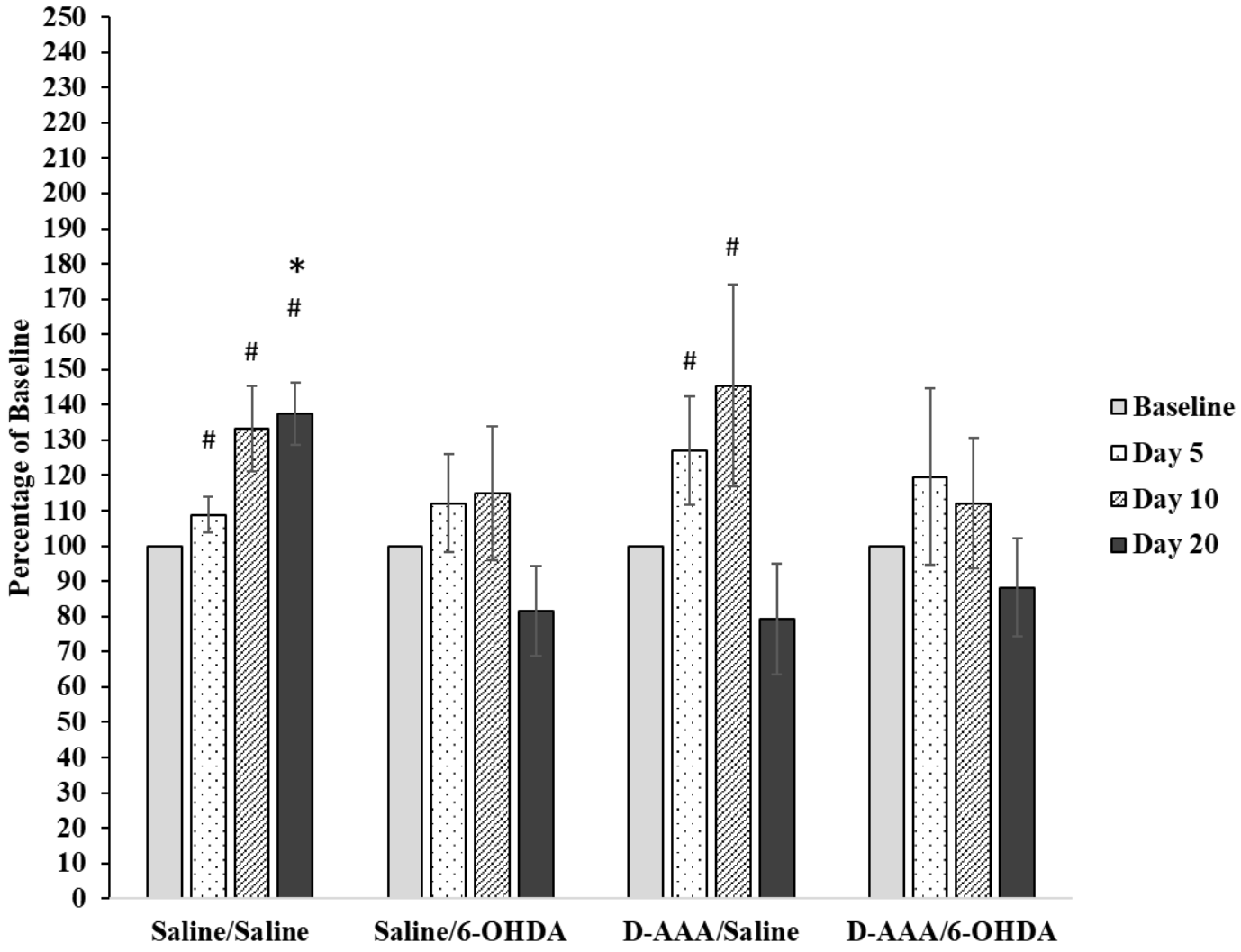

Figure 1. Mean latency to fall off Rotarod. The Rotarod is a motor learning task that tests an animal's balance, motor coordination, and strength. Four trials, each separated by 30 minutes, were performed for each animal at baseline, day 5, day 10 and day 20. The four trials were averaged per rat per timepoint and transformed into a percentage of baseline performance. * denotes significantly different than each other group at day 20. # denotes a significant difference in performance from baseline time for that group. Data expressed as the mean percentage of baseline performance with error bars as ± SEM

Digigait™ Gait Analysis System. A 2x2x4 repeated measures ANOVA was also conducted to assess the effect of a neurotoxin (6-OHDA vs. Saline) and gliotoxin (D-AAA vs. Saline) across time (baseline, day 5, day 10, day 20) on Digigait™ outcome measures. Briefly, the Digigait™ system produces a wide selection of gait parameters that are sensitive to changes in motor coordination (Mouse Specifics Inc., 2011). All outcome measures for the Digigait™ were expressed as a percentage of baseline performance.

Step angle coefficient of variation (CV) measures the variability in the step angle for each step, taking into account stance width and stride length (Mouse Specifics Inc., 2011). The interaction of neurotoxin x gliotoxin x time was not significant for forepaw step angle CV variable $F_{(3, 25)} = 2.490$, $p = 0.084$ *(Figure 2).* The interactions of neurotoxin x time ($F_{(3, 25)} = 1.650$, $p = 0.203$) and gliotoxin x time ($F_{(3, 25)} = 0.966$, $p = 0.424$) were also found to be not significant *(Figure 2)*. Finally, the main effect of time was not significant $F_{(3, 25)} = 1.758$, $p = 0.181$ (*Figure* 2). When we looked at the hindpaw step angle CV, the interaction of neurotoxin x gliotoxin x time was found to be not significant $F_{(3, 25)} = 1.176$, $p = 0.339$ (*Figure 3)*. There was also no significant interaction of either neurotoxin x time ($F_{(3, 25)} = 0.142$, $p = 0.934$) or gliotoxin x time ($F_{(3, 25)} = 1.906$, $p = 0.154$). Furthermore, the main effect of time was not significant $F_{(3, 25)} = 0.742$, $p = 0.537$ (*Figure 3).*

We also examined the ataxia coefficient which is another Digigait™ measure used as an index of the variability between steps, calculated for each limb (Mouse Specifics Inc., 2011). For the left forepaw the interaction of neurotoxin x gliotoxin x time was not significant $F_{(3, 25)} = 0.738$, $p = 0.539$ *(Figure 4)*. There were also no significant interactions for either the neurotoxin x time ($F_{(3, 25)} = 1.022$, $p = 0.400$) or gliotoxin x time ($F_{(3, 25)} = 1.118$, $p = 0.360$) (*Figure 4)*. Finally, the main effect of time was not significant $F_{(3, 25)} = 1.566$, $p = 0.223$ (*Figure 4).*When we looked at the

left hindpaw there was again no significant interaction of neurotoxin x gliotoxin x time $F_{(3, 25)}$ = 0.192, p = 0.901 (*Figure 5)*. There were also no interactions of neurotoxin x time ($F_{(3, 25)}$ = 0.292, p = 0.831) or gliotoxin x time ($F_{(3, 25)}$ =0.329, p = 0.804) and similarly, no significant main effect of time ($F_{(3, 25)}$ = 0.427, p = 0.735) (*Figure 5)*. For the right forepaw, the interaction of neurotoxin x gliotoxin x time was not significant $F_{(3, 25)}$ = 0.497, p = 0.688 (*Figure 6).* There were also no significant interactions for either neurotoxin x time ($F_{(3, 25)}$ = 1.254, p = 0.312) or gliotoxin x time ($F_{(3, 25)}$ =1.341, p = 0.284) (*Figure 6)*. In addition, the main effect of time was not significant $F_{(3, 25)}$ = 1.186, p = 0.335 (*Figure 6)*. Finally, when we looked at the right hindpaw ataxia coefficient the interaction of neurotoxin x gliotoxin x time was not significant $F_{(3, 25)}$ = 0.310, p = 0.818 (*Figure 7).* There was also no significant interaction for either neurotoxin x time ($F_{(3, 25)}$ = 0.915, p = 0.448) or gliotoxin time ($F_{(3, 25)}$ =0.037, p = 0.990) (*Figure 7)*. Similarly, the main effect of time was not significant $F_{(3, 25)}$ = 0.651, p = 0.590 (*Figure 7).*

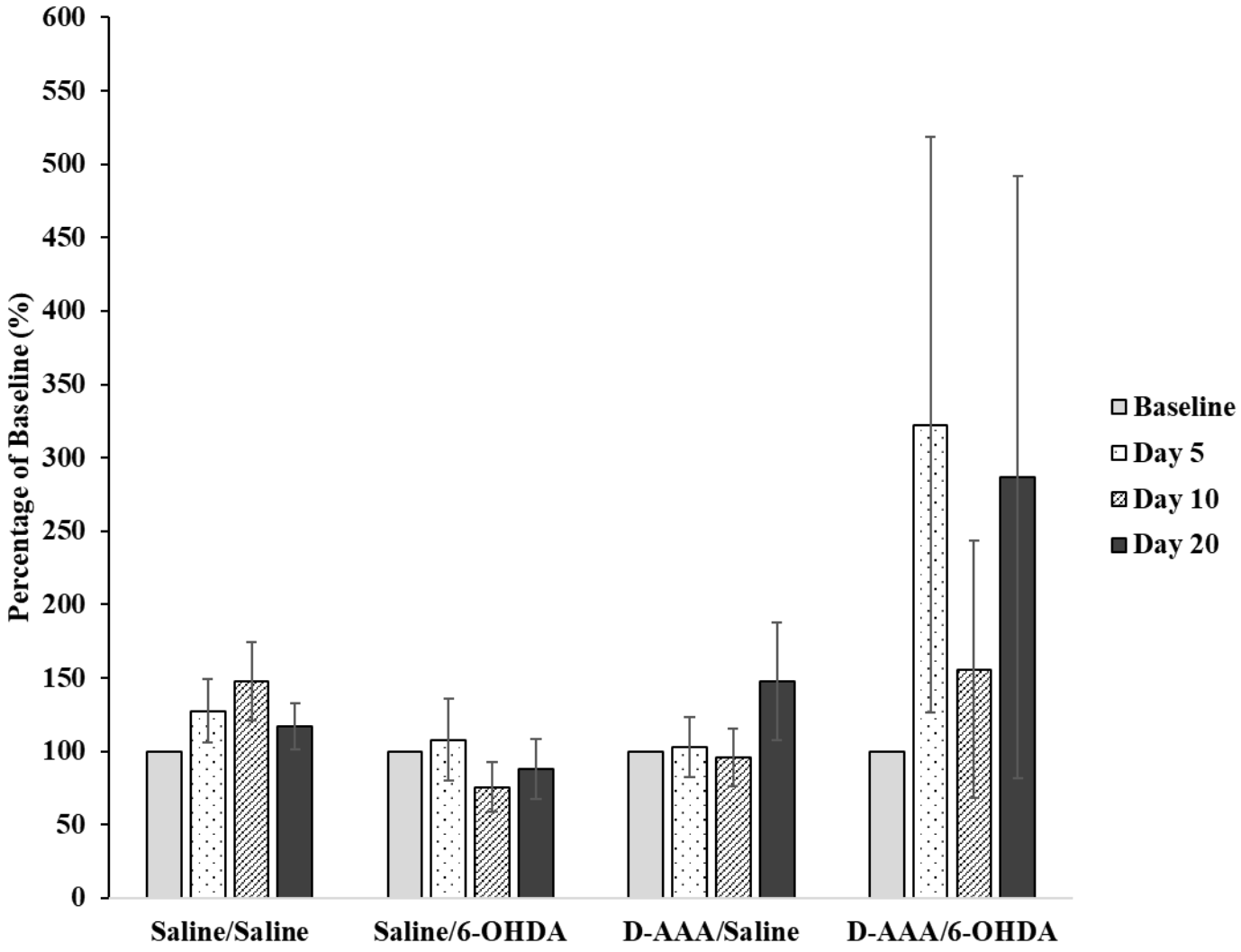

Figure 2. Forepaw step angle coefficient of variation. Animals were placed on the Digigait ™ and allowed to walk until a 3 second video of uninterrupted steps was obtained at baseline, day 5, day 10 and day 20. Forepaw step angle coefficient of variation is a measure of the variability in the step angle for each step, taking into account stance width and stride length (Mouse Specifics Inc., 2011) for the two forepaws. Raw data was transformed to a percentage of baseline performance and means were calculated from all animals per group, per timepoint. Data expressed as the mean percentage of baseline performance with error bars as ± SEM

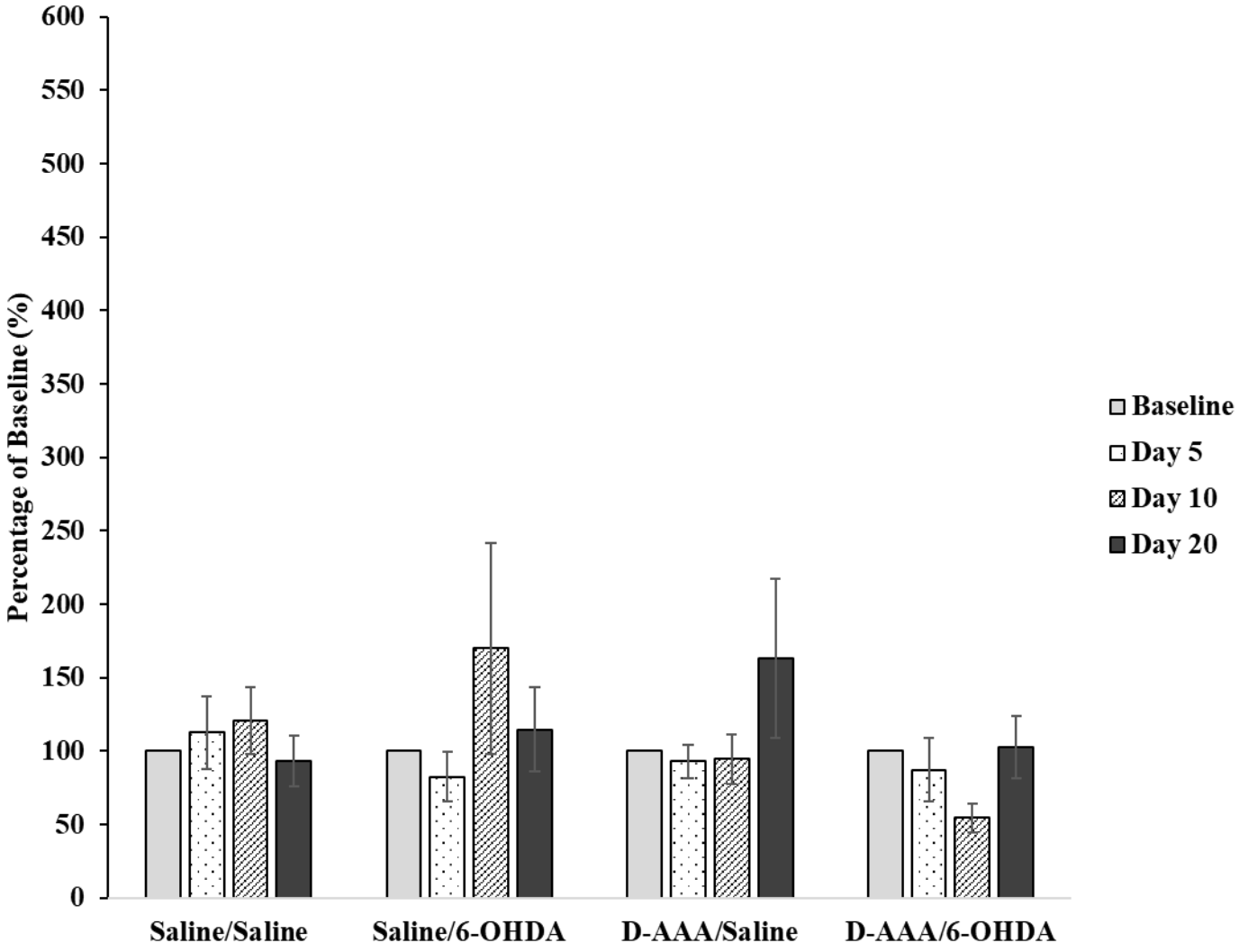

Figure 3. Hindpaw step angle coefficient of variation. Animals were placed on the Digigait ™ and allowed to walk until a 3 second video of uninterrupted steps was obtained at baseline, day 5, day 10 and day 20. Hindpaw step angle coefficient of variation is a measure of the variability in the step angle for each step, taking into account stance width and stride length (Mouse Specifics Inc., 2011) for the two hindpaws. Raw data was transformed to a percentage of baseline performance and means were calculated from all animals per group, per timepoint. Data expressed as the mean percentage of baseline performance with error bars as ± SEM

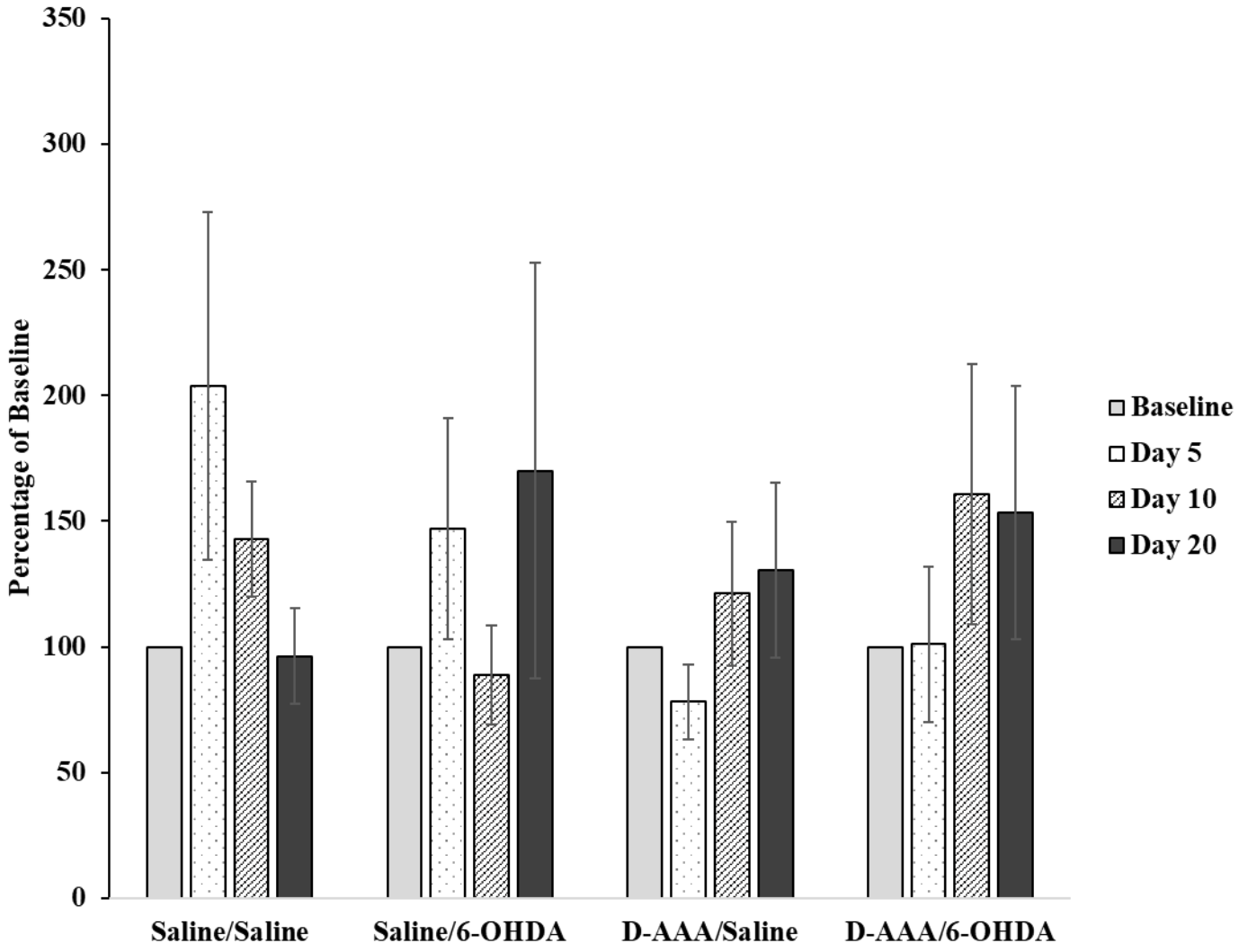

Figure 4. Left forepaw ataxia coefficient. Animals were placed on the Digigait ™ and allowed to walk until a 3 second video of uninterrupted steps was obtained at baseline, day 5, day 10 and day 20. Ataxia coefficient is an index of the variability between steps calculated for each limb (Mouse Specifics Inc., 2011). Raw data was transformed to a percentage of baseline performance and means were calculated from all animals per group, per timepoint. Data expressed as the mean percentage of baseline performance with error bars as ± SEM

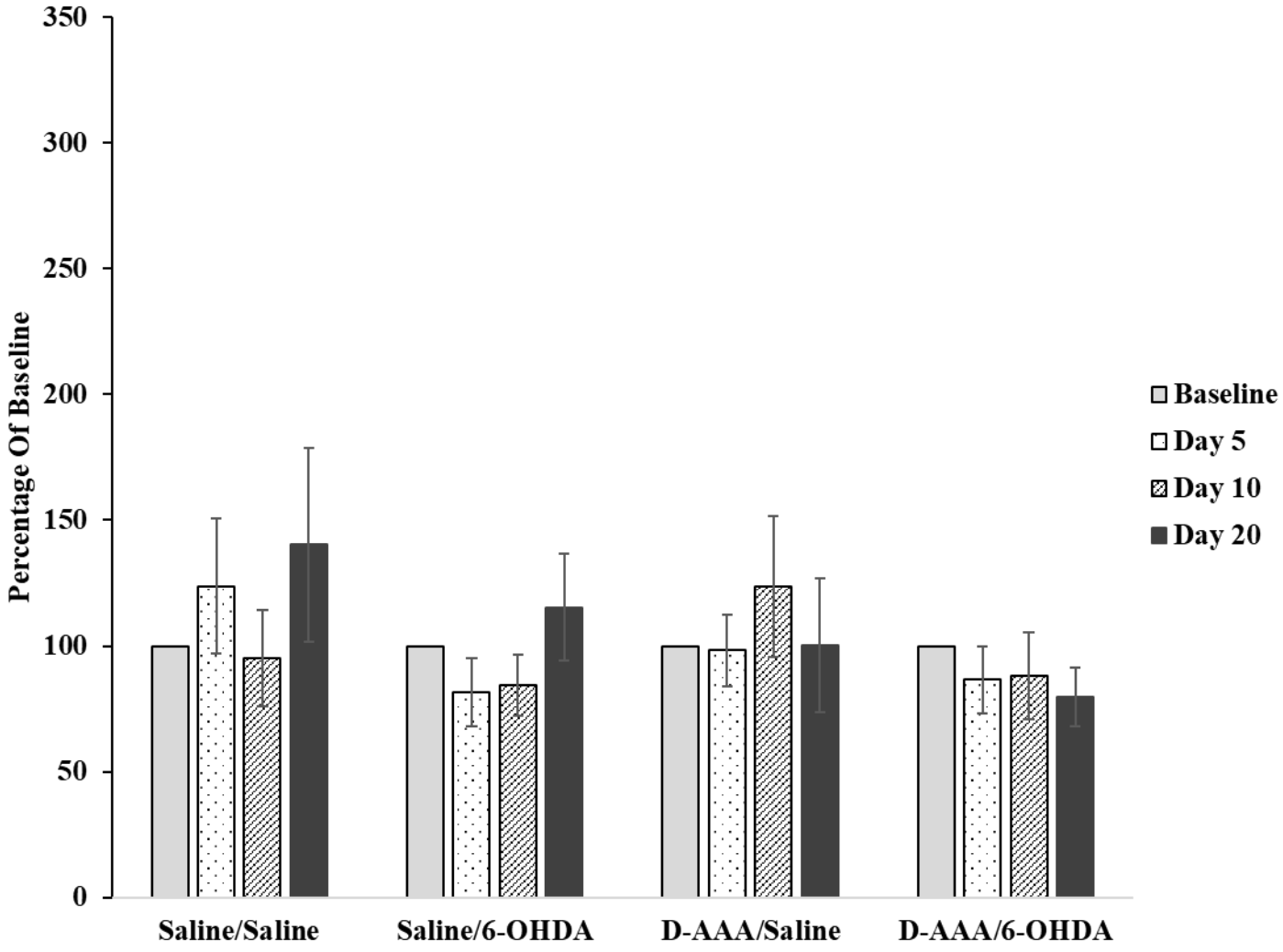

Figure 5. Left hindpaw ataxia coefficient. Animals were placed on the Digigait ™ and allowed to walk until a 3 second video of uninterrupted steps was obtained at baseline, day 5, day 10 and day 20. Ataxia coefficient is an index of the variability between steps calculated for each limb (Mouse Specifics Inc., 2011). Raw data was transformed to a percentage of baseline performance and means were calculated from all animals per group, per timepoint. Data expressed as the mean percentage of baseline performance with error bars as ± SEM

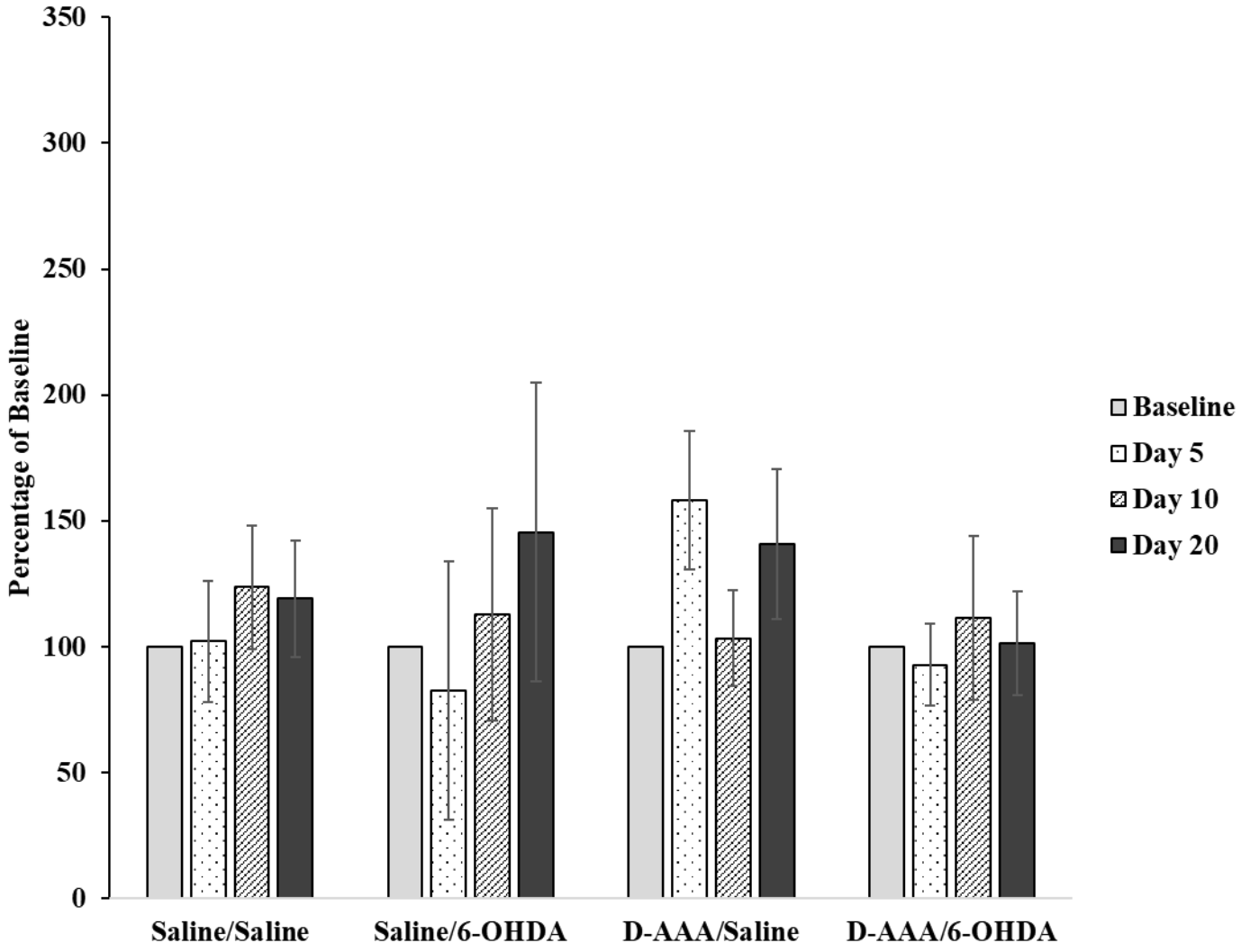

Figure 6. Right forepaw ataxia coefficient. Animals were placed on the Digigait ™ and allowed to walk until a 3 second video of uninterrupted steps was obtained at baseline, day 5, day 10 and day 20. Ataxia coefficient is an index of the variability between steps calculated for each limb (Mouse Specifics Inc., 2011). Raw data was transformed to a percentage of baseline performance and means were calculated from all animals per group, per timepoint. Data expressed as the mean percentage of baseline performance with error bars as ± SEM

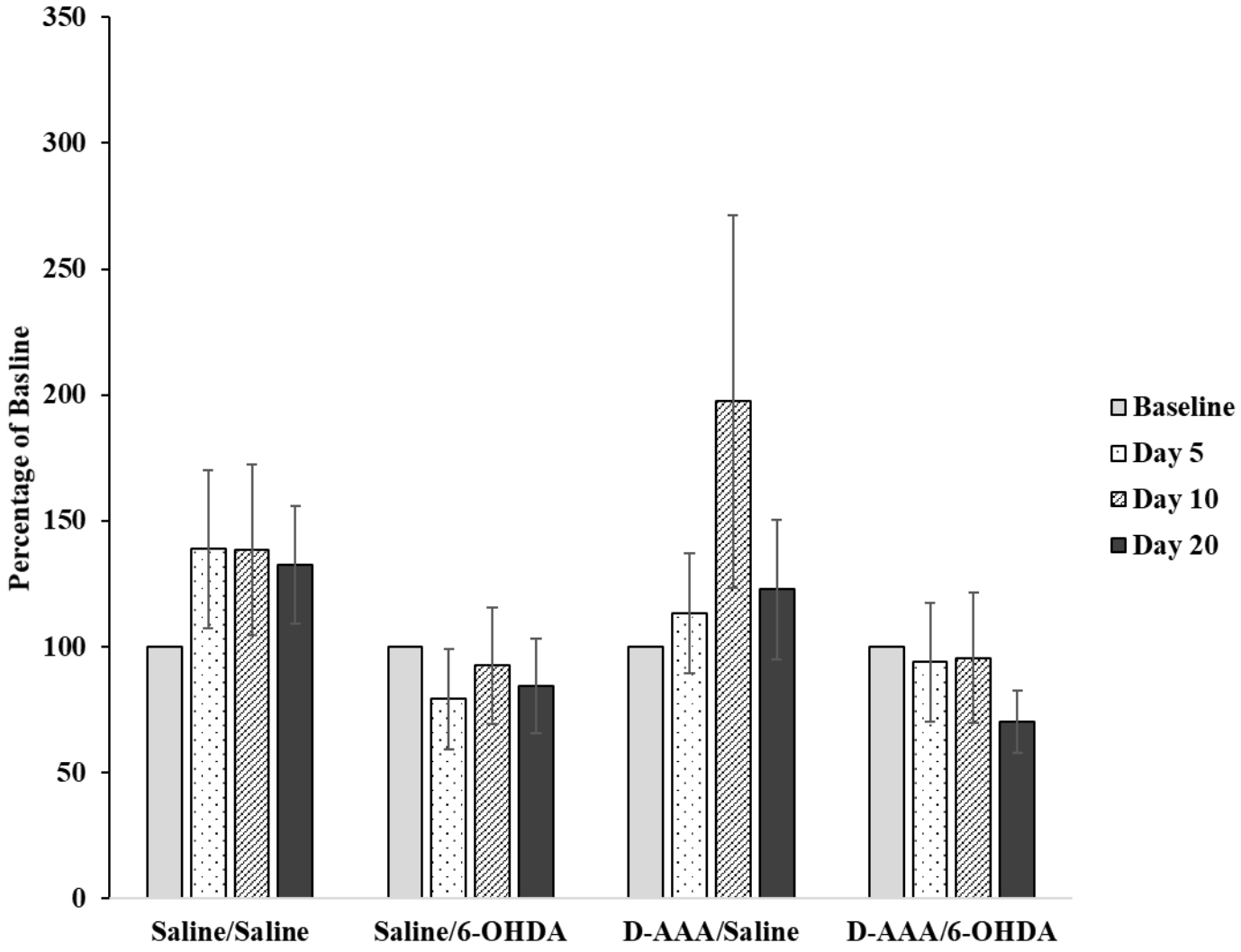

Figure 7. Right hindpaw ataxia coefficient. Animals were placed on the Digigait ™ and allowed to walk until a 3 second video of uninterrupted steps was obtained at baseline, day 5, day 10 and day 20. Ataxia coefficient is an index of the variability between steps calculated for each limb (Mouse Specifics Inc., 2011). Raw data was transformed to a percentage of baseline performance and means were calculated from all animals per group, per timepoint. Data expressed as the mean percentage of baseline performance with error bars as ± SEM

Immunohistochemical Analyses

TH Quantification. A 2x2 ANOVA was conducted to assess the effect of a neurotoxin (6-OHDA vs. Saline) and a gliotoxin (D-AAA vs. Saline) on the immunoreactivity (IR) of TH, a marker of DA cells. Results for THir revealed a statistically significant interaction between the neurotoxin and gliotoxin $F_{(3, 45)} = 6.930$, $p = 0.012$ (*Figure 8)*. Post hoc tests revealed that Saline/Saline controls had a higher THir when compared to all other groups ($p = < 0.01$) (*See Figure 10 for representative image).*

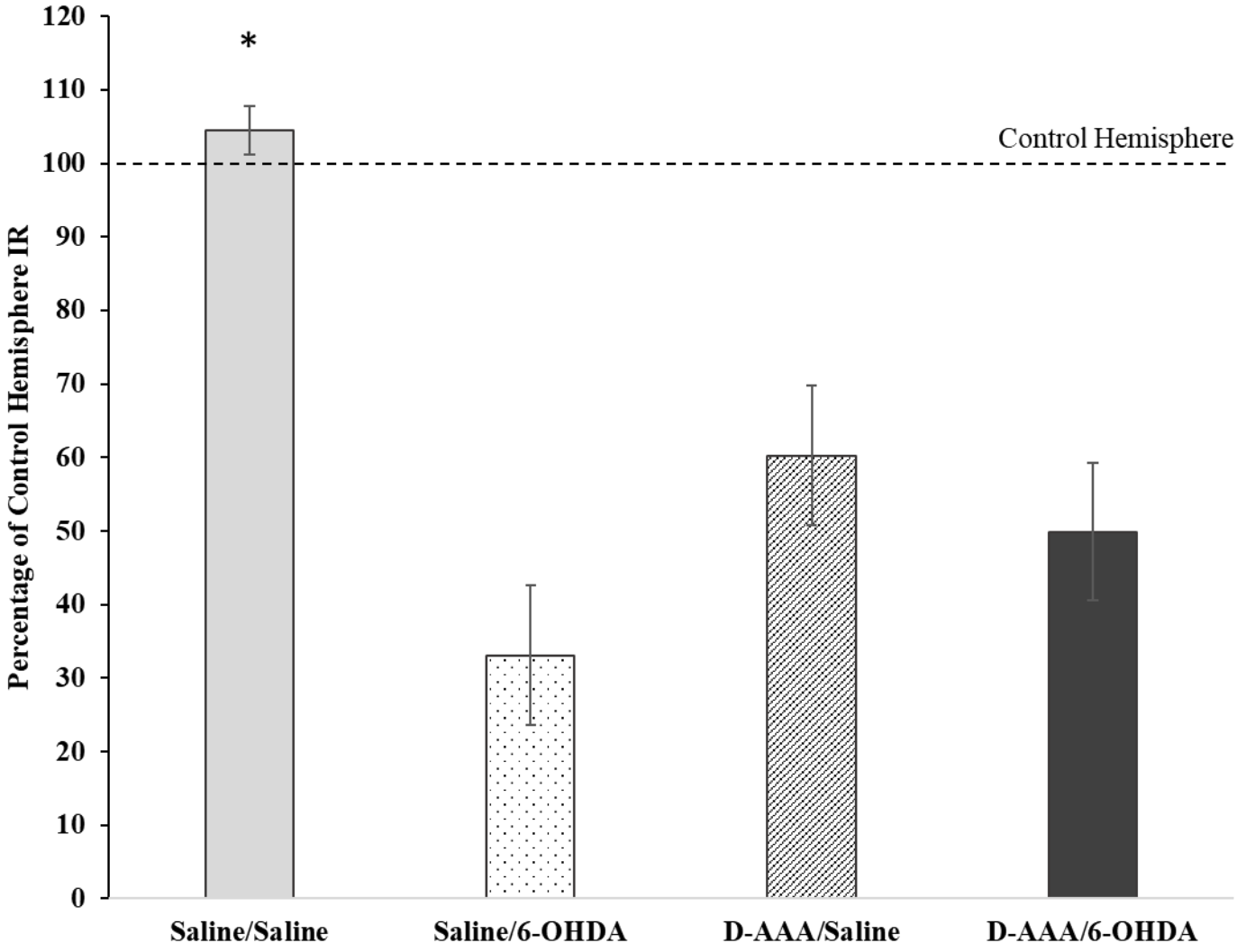

Figure 8. Tyrosine hydroxylase immunoreactivity. TH immunoreactivity in the SNc measured as a percentage of control hemisphere for all animals per group. TH immunoreactivity is a marker of DA cells and was measured using ImageJ to perform an optical density analysis. Optical density was obtained by creating regions of interest (ROI) of the SNc in both hemispheres and dividing the total fluorescence of each ROI by the area of each ROI. * denotes significantly different than each other group *(p = <0.05)*. Data expressed as the mean percentage of control hemisphere with error bars as ± SEM

GFAP Quantification. A 2x2 ANOVA was conducted to assess the effect of a neurotoxin (6-OHDA vs. Saline) and a gliotoxin (D-AAA vs. Saline) on the IR of GFAP, an astroglial cell marker. When GFAPir was examined, results indicated that there was a significant interaction between the neurotoxin and gliotoxin $F_{(3, 43)} = 4.131$, $p = 0.048$ (*Figure 9)*. Post hoc tests revelated that GFAPir was significantly lower in rats treated with both toxins when compared to rats that were treated with the gliotoxin alone ($p = < 0.01$) (*See Figure 10 for representative image)*.

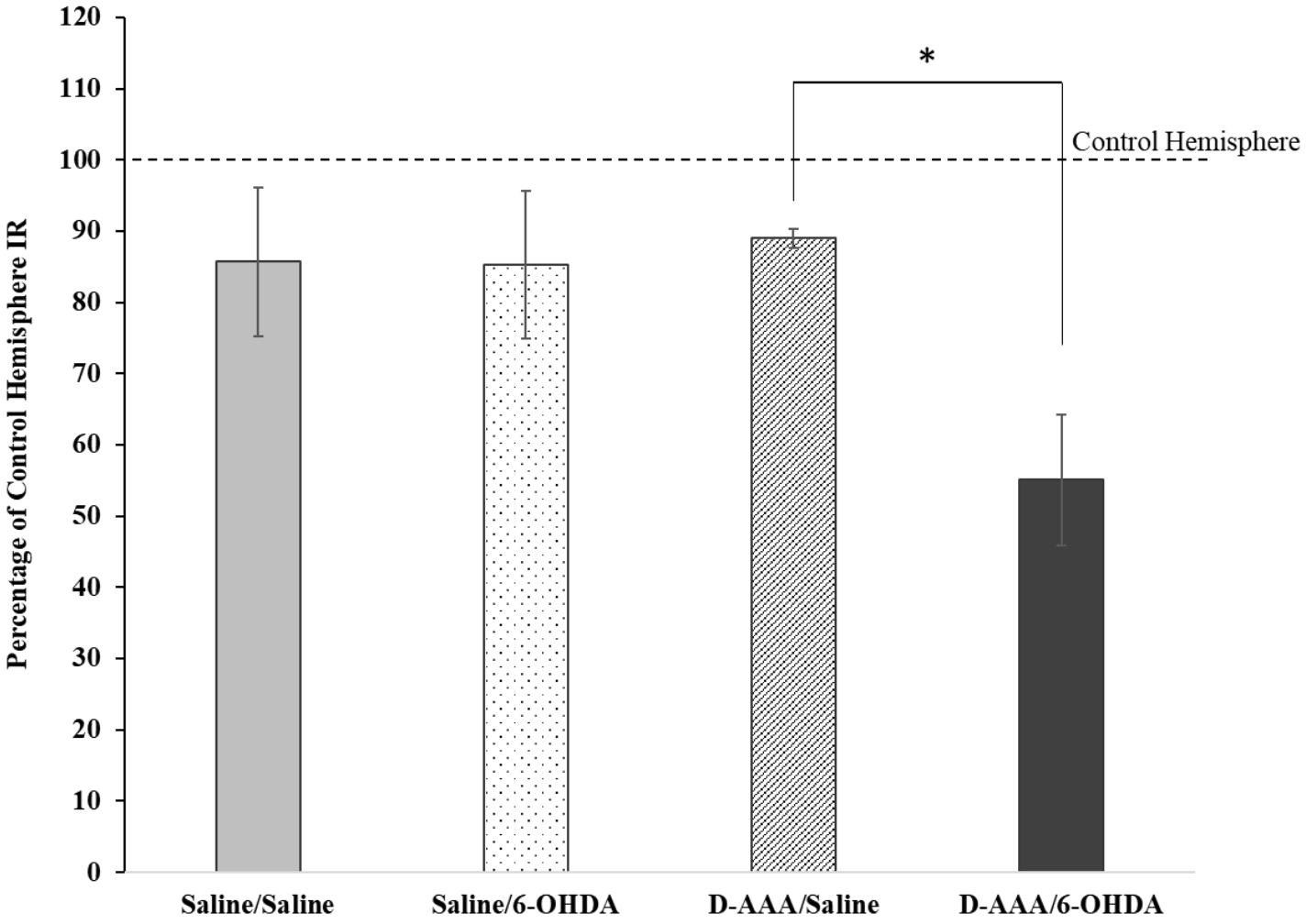

Figure 9. Glial fibrillary acidic protein immunoreactivity. GFAP immunoreactivity in the SNc measured as a percentage of control hemisphere for all animals per group. GFAP immunoreactivity is a marker of DA cells and was measured using ImageJ to perform an optical density analysis. Optical density was obtained by creating ROI of the SNc in both hemispheres and dividing the total fluorescence of each ROI by the area of each ROI. * denotes groups are significantly different from each other *(p* = <0.05). Data expressed as the mean percentage of control hemisphere with error bars as ± SEM

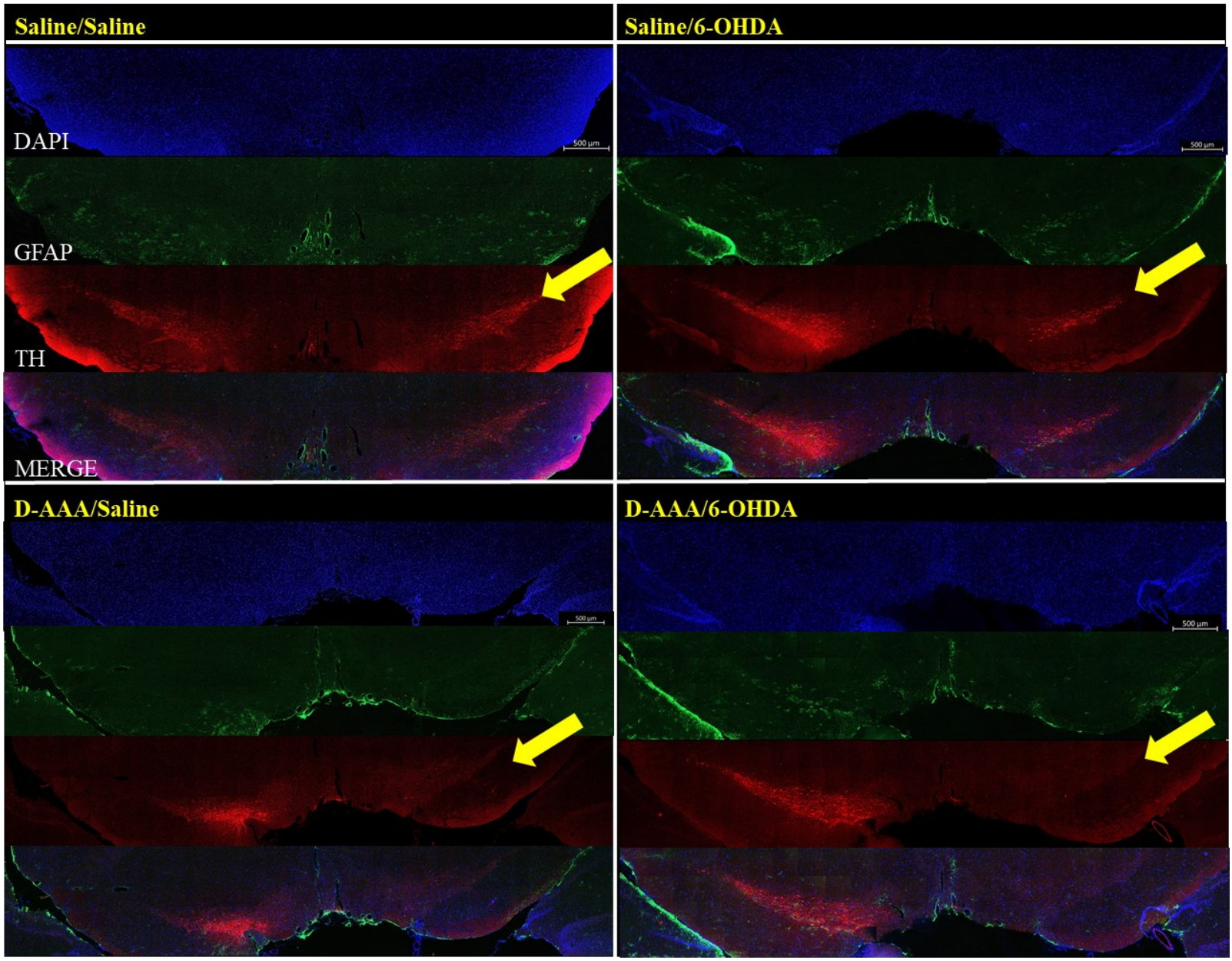

Figure 10. Representative image of all groups. Tiled images of the SNc taken at 20x using Zeiss LSM 800 confocal microscope. Stakes were set to identify total area to image and autofocus was set to focus using the DAPI channel for each individual tile. DAPI is an overall marker of cells, TH is a marker of DA cells, and GFAP is a marker of astrocytes. The yellow arrow identifies the lesioned hemisphere for the TH channel.

Correlations

Pearson correlations. To determine the relationship between TH or GFAP IR and all behavioural outcomes, Pearson correlation coefficients were calculated. Interestingly, THir was significantly correlated with latency to fall off the rotarod at day 20, r = 0.325, $p = < 0.05$ (*Figure 11*) (*See Table 3 for the complete correlation table*).

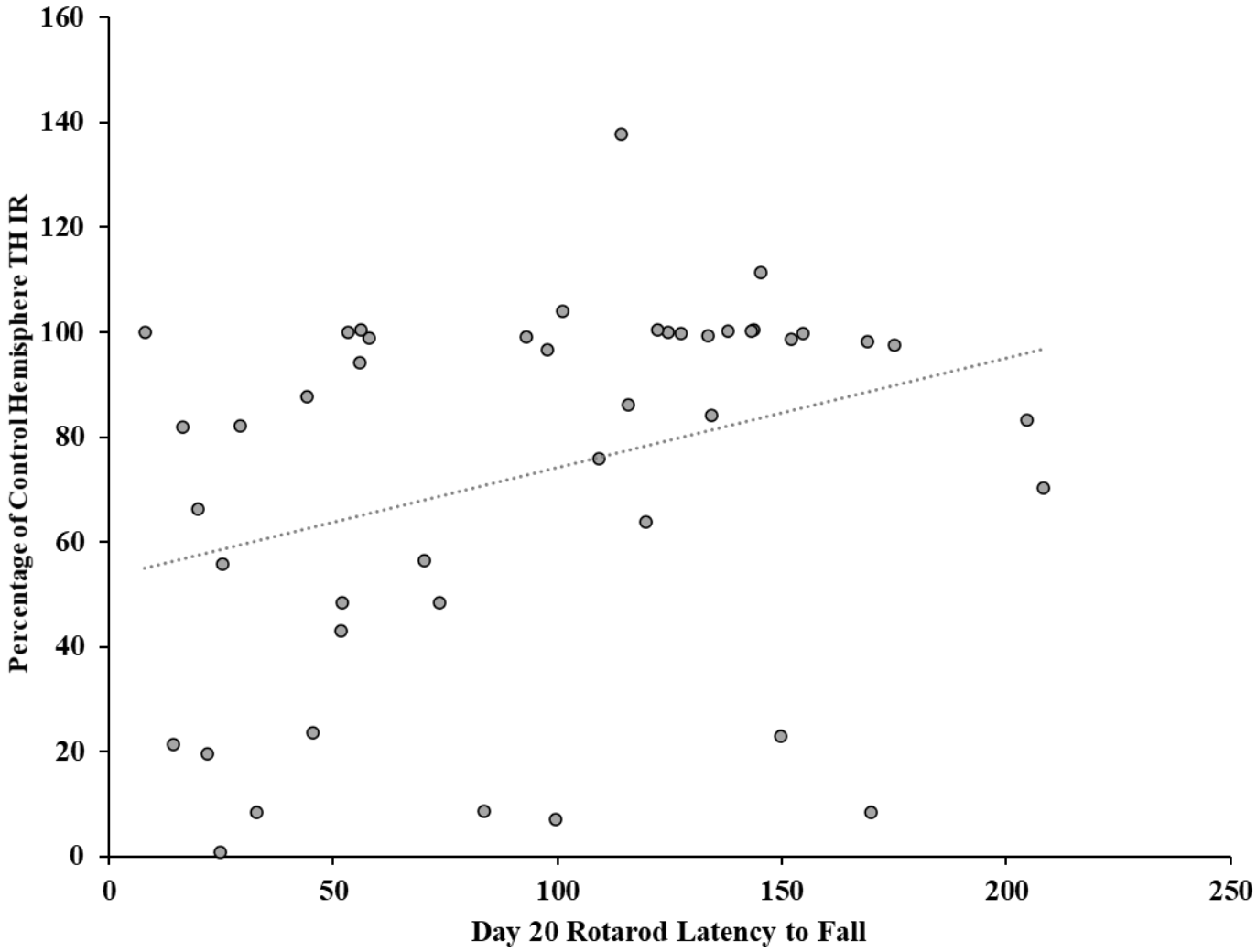

Figure 11. Correlation between TH immunoreactivity and Day 20 rotarod. TH immunoreactivity in the SNc measured as a percentage of control hemisphere for all animals per group. TH immunoreactivity is a marker of DA cells and was measured using ImageJ to perform an optical density analysis. Optical density was obtained by creating ROI of the SNc in both hemispheres and dividing the total fluorescence of each ROI by the area of each ROI. The Rotarod is a motor learning task that tests an animal's balance, motor coordination, and strength. Four trials, each separated by 30 minutes, were performed for each animal on day 20 and were averaged per rat per timepoint then transformed into a percentage of baseline performance. A significant correlation was found, r = 0.325 (*p = < 0.05).*

Table 4. Pearson correlations between TH and GFAP and behavioural data.

	1	2
1. TH (% of control)	1	
2. GFAP (% of control)	0.185	1
3. Rotarod (Day 20)	0.325*	0.036
4. Forepaw Step Angle CV (Day 20)	0.055	-0.147
5. Hindpaw Step Angle CV (Day 20)	-0.153	0.136
6. Left Forepaw Ataxia Coefficient (Day 20)	0.104	-0.124
7. Left Hindpaw Ataxia Coefficient (Day 20)	0.184	0.102
8. Right Forepaw Ataxia Coefficient (Day 20)	-0.232	0.224
9. Right Hindpaw Ataxia Coefficient (Day 20)	0.050	0.097

*** Correlation significant where $p < 0.05$ (2-tailed)**

Discussion

The objective of the current study was to examine how DA cells react to the sudden loss of astrocytes in the SNc, and to broadly examine whether the role of astrocytes in PD extends beyond a secondary, reactive role to direct involvement in the induction of neurodegeneration. To achieve this, we have employed a striatal 6-OHDA lesion and a SNc astrocytic lesion both individually and together and examined the effects on motor behaviour and DA cell degeneration in the SNc.

Although it is well-documented that exposing SNc DA cells to a toxin will induce motor deficits similar to that observed in PD, the present study is the first to demonstrate that the loss of astroglia in the SNc is sufficient to induce loss of surrounding TH^+ cells and deficits in related motor behaviour. Incredibly, only a small loss of astrocytes is required- as we only induced a 10-15% loss of astrocytes in the SNc. Many studies that examine astrocytes' role in PD focus on how they can promote neuronal survival (Yun et al., 2018; Kostuk et al., 2019), making these results especially exciting, as they demonstrate that astrocytes are in fact critical for the survival of the surrounding neurons in basal conditions. The notion that astrocytes are the driver of pathological disease (Barres, 2008; Sofroniew and Vinters, 2010; Liddelow and Sofroniew, 2019) is supported by our observation that the loss of astrocytes lead to the same deficits as if the neurons were directly lesioned themselves

6-OHDA has been used for many years as a model of PD; the paradigm has been well-delineated and it is easy to produce a consistent and specific DA cell lesion (Ungerstedt, 1968). The intrastriatal injection of 6-OHDA leads to the retrograde degeneration of DA cells in the SNc by being taken up by the terminals in the striatum and autooxidizing, causing a massive increase in ROS and interfering with the mitochondrial respiration chain (Glinka et al., 1997; Rodriguez-

Pallares et al., 2007). This means that there is a loss of DA terminals in the striatum as soon as 48 hours after injection, but it takes up to two weeks for DA cell death in the SNc and for the subsequent behavioural deficits to present (Rodriguez-Pallares et al., 2007). This pattern and mechanism of degeneration closely mimics the observed pattern and mechanisms of DA cell degeneration that is observed in the midbrain of humans with PD (Lee et al., 1996; Blandini et al., 2008). The behavioural deficits that occur as a result of the lesion have been well documented (Su et al., 2018). Our results on the rotarod are in line with what is commonly seen in the literature for the corresponding dose of 6-OHDA (Su et al., 2018). We observed the Saline/Saline controls continuously increasing their performance throughout the timepoints, having their highest latency to fall on day 20, indicating an ability to learn and improve on the task as would be expected in a control condition. The D-AAA/Saline group also exhibited increasing performance through to day 10, which presumably is due to the effect of the glial lesion on dopamine cell viability (as supported by THir levels) and subsequent motor performance. Overall, we observed that animals who received either the gliotoxin alone, or both the gliotoxin and neurotoxin had a significantly lower latency to fall of the rotarod at day 20 than the saline controls did. It is interesting to see that the gliotoxin alone led to a similar level of motor deficit, but not unexpected given that we observed a reduction in TH^+ cell density similar to what we observed in the neurotoxin group.

The decrease in TH^+ cell density in response to a single injection of the gliotoxin is especially interesting, suggesting that DA cells in the SNc are vulnerable to even a small loss of astrocytes. The reason for this susceptibility is unknown, however, DA cells are especially prone to oxidative stress, as DA itself is easily oxidized, and the metabolism of DA regularly produces hydrogen peroxide (Meiser et al., 2013). Astrocytes are able to protect surrounding neurons from ROS throughout the brain (Drukarch et al., 1998), specifically being important for the

detoxification of hydrogen peroxide through glutathione peroxidase and catalase activity (Desagher et al., 1996; Dringen and Hamprecht, 1997; Dringen et al., 2000). While the neurons themselves have some ability to clear hydrogen peroxide, the capacity and efficiency is far less than what is seen in astrocytes (Dringen et al., 1999). It is possible that the small loss of astrocytes induced by the gliotoxin was sufficient to overwhelm the remaining cells' ability to deal with the production of ROS and hydrogen peroxide, leading the degeneration of DA cells we observed.

In both our analysis of THir and GFAPir, we observed a significant interaction between 6-OHDA and D-AAA. Specifically, in our analysis of GFAPir, we observed the interaction of the neurotoxin and the gliotoxin resulted in a significant decrease in the amount of GFAPir. While we expected the combination of the neurotoxin and gliotoxin to result in a significant decrease in THir through the increased amount of oxidative stress (Glinka et al., 1997; Rodriguez-Pallares et al., 2007) coupled with the decrease in the ability to manage it (Desagher et al., 1996; Dringen and Hamprecht, 1997; Drukarch et al., 1998; Dringen et al., 1999, 2000), we did not expect the same to occur for GFAP. It has been shown that 6-OHDA can inhibit calcium signalling by interfering with purinergic mediated activation of transient receptor potential channel 3 (TRPC3), preventing the astrocytes from communicating and leading to a suppressed reaction in response to the toxin (Streifel et al., 2014). This suppressed reaction could leave astrocytes themselves vulnerable to the oxidative damage that is being caused by the 6-OHDA, given that they are the main line of defense against it.

We observed a significant decrease in $GFAP^+$ cells in response to the combination of the neurotoxin and gliotoxin, but not from either one on their own. While GFAP has been the de-facto marker of astrocytes for many years and is useful in assessing reactivity (Messing and Brenner, 2020), its use as a proxy for the number of astrocytes is limited and at times, incorrect. GFAP is

only expressed in about half of all astrocytes at a given time (Simard et al., 2018), and since it is a cytoskeletal protein, its expression is dynamically regulated (Hol and Pekny, 2015; Lowery et al., 2015). Only 40-50% of cortical astrocytes express GFAP and the percentage fluctuates greatly between regions, age, state amongst other variables. For these reasons, it is likely that we are missing an entire population of astrocytes when performing the analysis, meaning our findings regarding the number of astrocytes must be interpreted carefully. For example, a decrease in GFAP expression may simply indicate that the protein has been downregulated and not that the number of astrocytes has changed. A specific pan-astrocytic marker with stable expression (Simard et al., 2018) such as aldehyde dehydrogenase 1 family, member L1 (Aldh1L1) (Cahoy et al., 2008) should be used in future studies to accurately identify changes in the astrocyte population of the SNc. In addition, evaluation of cell death markers in astrocytes would directly assess whether there is a loss of cells, albeit the transient nature of cell death markers renders it difficult to capture at the time point we assessed in the current study.

A large number of studies have demonstrated exciting cross-talk between glial cells in pathological states, including PD (Liddelow et al., 2017; Clarke et al., 2018; Kuter et al., 2018; Joshi et al., 2019; O'Neill et al., 2019). Microglial activation is known to induce a neurotoxic astrocytic phenotype via IL-1α, TNF-α and C1q (Liddelow et al., 2017; Joshi et al., 2019). It is also well documented, that microglia become activated, as defined by an increase in CD11b staining, in response to 6-OHDA (Walsh et al., 2011; Stott and Barker, 2014), suggesting the presence of both activated microglia and neurotoxic astrocytes in the tissues we collected. Interestingly, it has been shown that an increase in IL-1β, a pro-inflammatory cytokine that is secreted by activated microglia (Sousa et al., 2018), increases DA cell susceptibility to degeneration by 6-OHDA. In contrary to this, astrocytic death has been demonstrated to attenuate

microgliosis, which in turn, provides a protective effect on the surrounding DA cells (O'Neill et al., 2019). While we did not examine microglia in this study, it stands to reason that our manipulations did have some effect on them, and that effect may have contributed to our results in some way. Future studies might explore this extensive cross-talk between neurons, astrocytes, and microglia to help further understand how PD might progress.

Our use of the Digigait™ and the associated outcome measures did not provide much insight into the behavioural deficits caused by the manipulations. While some measures trended towards significance, the majority of the measures explored were plagued by high variabilities. This high amount of variability in about 30% of gait parameters has been noted to occur in control animals (Zhan et al., 2019), so it is unsurprising that we encountered this in our data.. Interestingly, a study by Boix *et al.* (2018), examined the difference in gait parameters between a medial forebrain (MFB) 6-OHDA lesion and a striatal 6-OHDA lesion, similar to the one used in the current study. They found that automated gait analysis was able to accurately track motor deficits in the MFB lesioned animals but did not track them in the animals who received the striatal 6-OHDA lesion. They suggested that the difference could be due to the striatal lesion causing much less SNc TH^+ cell loss than the MFB lesion, as they also observed TH^+ cell loss correlating with behavioural measures (Boix et al., 2018). In future studies using a striatal 6-OHDA, it would appear that other commonly used motor behavioural tests such as amphetamine- or apomorphine-induced rotations are more sensitive to changes in TH^+ cell density in the SNc (Lee et al., 1996; Su et al., 2018; Miyanishi et al., 2019), and should be utilized in favour of automated gait analysis.

The work that comprised this research thesis had the objective of determining what role astrocytes may play in the early stages of PD, to help develop our understanding of the disease and how it may be treated. We have demonstrated that a modest loss of astrocytes in the SNc is

sufficient to induce a TH^+ cell loss that is not only consistent with our dose of 6-OHDA, but also produces motor deficits that are consistent with the 6-OHDA lesion. Our findings mark a novel role for astrocytes as primary players in neuronal degeneration and support the growing evidence critical roles of glia in addition to neurons when studying PD as well as other neurodegenerative diseases. While this study is a good first step, future directions should focus on using a model of PD that more closely mimics what is seen in humans, such as a humanized α-SYN model. By examining the role of astrocytes in ever more complex and valid models of PD, hopefully new avenues for effective drug treatments may present themselves.

References:

Abounit S, Bousset L, Loria F, Zhu S, de Chaumont F, Pieri L, Olivo-Marin J-C, Melki R, Zurzolo C (2016) Tunneling nanotubes spread fibrillar α-synuclein by intercellular trafficking of lysosomes. EMBO J 35:2120–2138.

Alilain WJ, Horn KP, Hu H, Dick TE, Silver J (2011) Functional regeneration of respiratory pathways after spinal cord injury. Nature 475:196–200.

Allen NJ, Barres BA (2009) Glia — more than just brain glue. Nature 457:675–677.

Anderson MA, Burda JE, Ren Y, Ao Y, O'Shea TM, Kawaguchi R, Coppola G, Khakh BS, Deming TJ, Sofroniew M V (2016) Astrocyte scar formation aids central nervous system axon regeneration. Nature 532:195–200.

Andres-Mateos E, Perier C, Zhang L, Blanchard-Fillion B, Greco TM, Thomas B, Ko HS, Sasaki M, Ischiropoulos H, Przedborski S, Dawson TM, Dawson VL (2007) DJ-1 gene deletion reveals that DJ-1 is an atypical peroxiredoxin-like peroxidase. Proc Natl Acad Sci 104:14807–14812.

Armbruster M, Hanson E, Dulla CG (2016) Glutamate Clearance Is Locally Modulated by Presynaptic Neuronal Activity in the Cerebral Cortex. J Neurosci 36:10404–10415.

Ashley AK, Hinds AI, Hanneman WH, Tjalkens RB, Legare ME (2016) DJ-1 mutation decreases astroglial release of inflammatory mediators. Neurotoxicology 52:198–203.

Attwell D, Buchan AM, Charpak S, Lauritzen M, Macvicar BA, Newman EA (2010) Glial and neuronal control of brain blood flow. Nature 468:232–243.

Banasr M, Duman RS (2008) Glial Loss in the Prefrontal Cortex Is Sufficient to Induce Depressive-like Behaviors. Biol Psychiatry 64:863–870.

Bandopadhyay R et al. (2004) The expression of DJ-1 (PARK7) in normal human CNS and idiopathic Parkinson's disease. Brain 127:420–430.

Barres BA (2008) The Mystery and Magic of Glia: A Perspective on Their Roles in Health and Disease. Neuron 60:430–440.

Bazelon M, Fenichel GM, Randall J (1967) Studies on neuromelanin. I. A melanin system in the human adult brainstem. Neurology 17:521.

Bekar LK, He W, Nedergaard M (2008) Locus coeruleus alpha-adrenergic-mediated activation of cortical astrocytes in vivo. Cereb Cortex 18:2789–2795.

Blandini F, Armentero MT, Martignoni E (2008) The 6-hydroxydopamine model: News from the past. Park Relat Disord 14.

Blesa J, Trigo-Damas I, Quiroga-Varela A, Jackson-Lewis VR (2015) Oxidative stress and Parkinson's disease. Front Neuroanat 9.

Boix J, von Hieber D, Connor B (2018) Gait analysis for early detection of motor symptoms in the 6-ohda rat model of parkinson's disease. Front Behav Neurosci 12:39.

Bonello F, Hassoun S-M, Mouton-Liger F, Shin YS, Muscat A, Tesson C, Lesage S, Beart PM, Brice A, Krupp J, Corvol J-C, Corti O (2019) LRRK2 impairs PINK1/Parkin-dependent mitophagy via its kinase activity: pathologic insights into Parkinson's disease. Hum Mol Genet 28:1645–1660.

Bonifati V, Rizzu P, van Baren MJ, Schaap O, Breedveld GJ, Krieger E, Dekker MCJ, Squitieri F, Ibanez P, Joosse M, van Dongen JW, Vanacore N, van Swieten JC, Brice A, Meco G, van Duijn CM, Oostra BA, Heutink P (2003) Mutations in the DJ-1 Gene Associated with Autosomal Recessive Early-Onset Parkinsonism. Science (80-) 299:256–259.

Booth HDE, Hirst WD, Wade-Martins R (2017) The Role of Astrocyte Dysfunction in Parkinson's Disease Pathogenesis. Trends Neurosci 40:358–370.

Braak H, Ghebremedhin E, Rüb U, Bratzke H, Del Tredici K (2004) Stages in the development of Parkinson's disease-related pathology. Cell Tissue Res 318:121–134.

Braak H, Tredici K Del, Rüb U, De Vos RAI, Jansen Steur ENH, Braak E (2003) Staging of brain pathology related to sporadic Parkinson's disease. Neurobiol Aging 24:197–211.

Bradbury EJ, Moon LDF, Popat RJ, King VR, Bennett GS, Patel PN, Fawcett JW, McMahon SB (2002) Chondroitinase ABC promotes functional recovery after spinal cord injury. Nature 416:636–640.

Brown DR, Kretzschmar HA (1998) The glio-toxic mechanism of α-aminoadipic acid on cultured astrocytes. J Neurocytol 27:109–118.

Cahoy JD, Emery B, Kaushal A, Foo LC, Zamanian JL, Christopherson KS, Xing Y, Lubischer JL, Krieg PA, Krupenko SA, Thompson WJ, Barres BA (2008) A transcriptome database for astrocytes, neurons, and oligodendrocytes: A new resource for understanding brain development and function. J Neurosci 28:264–278.

Cheng H-C, Ulane CM, Burke RE (2010) Clinical progression in Parkinson disease and the neurobiology of axons. Ann Neurol 67:715–725.

Choi D-J, Eun J-H, Kim BG, Jou I, Park SM, Joe E-H (2018) A Parkinson's disease gene, DJ-1, repairs brain injury through Sox9 stabilization and astrogliosis. Glia 66:445–458.

Christopherson KS, Ullian EM, Stokes CCA, Mullowney CE, Hell JW, Agah A, Lawler J, Mosher DF, Bornstein P, Barres BA (2005) Thrombospondins Are Astrocyte-Secreted Proteins that Promote CNS Synaptogenesis. Cell 120:421–433.

Clarke LE, Liddelow SA, Chakraborty C, Münch AE, Heiman M, Barres BA (2018) Normal aging induces A1-like astrocyte reactivity. Proc Natl Acad Sci 115:E1896–E1905.

Colodner KJ, Montana RA, Anthony DC, Folkerth RD, De Girolami U, Feany MB (2005) Proliferative Potential of Human Astrocytes. J Neuropathol Exp Neurol 64:163–169.

Daneman R, Prat A (2015) The blood-brain barrier. Cold Spring Harb Perspect Biol 7:a020412.

Datta I, Ganapathy K, Razdan R, Bhonde R (2018) Location and Number of Astrocytes Determine Dopaminergic Neuron Survival and Function Under 6-OHDA Stress Mediated Through Differential BDNF Release. Mol Neurobiol 55:5505–5525.

Daubner SC, Le T, Wang S (2011) Tyrosine hydroxylase and regulation of dopamine synthesis. Arch Biochem Biophys 508:1–12.

De Miranda BR, Rocha EM, Bai Q, El Ayadi A, Hinkle D, Burton EA, Timothy Greenamyre J (2018) Astrocyte-specific DJ-1 overexpression protects against rotenone-induced neurotoxicity in a rat model of Parkinson's disease. Neurobiol Dis 115:101–114.

De Pittà M, Brunel N, Volterra A (2016) Astrocytes: Orchestrating synaptic plasticity? Neuroscience 323:43–61.

Desagher S, Glowinski J, Premont J (1996) Astrocytes protect neurons from hydrogen peroxide toxicity. J Neurosci 16:2553–2562.

Dringen R, Gutterer JM, Hirrlinger J (2000) Glutathione metabolism in brain: Metabolic interaction between astrocytes and neurons in the defense against reactive oxygen species. Eur J Biochem 267:4912–4916.

Dringen R, Hamprecht B (1997) Involvement of glutathione peroxidase and catalase in the disposal of exogenous hydrogen peroxide by cultured astroglial cells. Brain Res 759:67–75.

Dringen R, Kussmaul L, Gutterer JM, Hirrlinger J, Hamprecht B (1999) The glutathione system of peroxide detoxification is less efficient in neurons than in astroglial cells. J Neurochem 72:2523–2530.

Drukarch B, Schepens E, Stoof JC, Langeveld CH, Van Muiswinkel FL (1998) Astrocyte-enhanced neuronal survival is mediated by scavenging of extracellular reactive oxygen species. Free Radic Biol Med 25:217–220.

Duffy PE, Tennyson VM (1965) Phase and Electron Microscopic Observations of Lewy Bodies and Melanin Granules in the Substantia Nigra and Locus Coeruleus in Parkinson's Disease. J Neuropathol Exp Neurol 24:398–414.

Dvorzhak A, Melnick I, Grantyn R (2018) Astrocytes and presynaptic plasticity in the striatum: Evidence and unanswered questions. Brain Res Bull 136:17–25.

Ehringer H, Hornykiewicz O (1960) Distribution of noradrenaline and dopamine (3-hydroxytyramine) in the human brain and their behavior in diseases of the extrapyramidal system. Klin Wochenschr 38:1236.

Engelhardt E, Gomes M da M (2017) Lewy and his inclusion bodies: Discovery and rejection. Dement Neuropsychol 11:198–201.

Fan X, Agrid Y (2018) At the Origin of the History of Glia. Neuroscience 385:255–271.

Faulkner JR, Herrmann JE, Woo MJ, Tansey KE, Doan NB, Sofroniew M V (2004) Reactive Astrocytes Protect Tissue and Preserve Function after Spinal Cord Injury. J Neurosci 24:2143–2155.

Fellin T, Halassa MM, Terunuma M, Succol F, Takano H, Frank M, Moss SJ, Haydon PG (2009) Endogenous nonneuronal modulators of synaptic transmission control cortical slow oscillations in vivo. Proc Natl Acad Sci U S A 106:15037–15042.

Fitch MT, Silver J (2008) CNS injury, glial scars, and inflammation: Inhibitory extracellular

matrices and regeneration failure. Exp Neurol 209:294–301.

Freitas-Andrade M, Naus CC (2016) Astrocytes in neuroprotection and neurodegeneration: The role of connexin43 and pannexin1. Neuroscience 323:207–221.

Giguère N, Delignat-Lavaud B, Herborg F, Voisin A, Li Y, Jacquemet V, Anand-Srivastava M, Gether U, Giros B, Trudeau L-É (2019) Increased vulnerability of nigral dopamine neurons after expansion of their axonal arborization size through D2 dopamine receptor conditional knockout Petrou S, ed. PLOS Genet 15:e1008352.

Gilks WP, Abou-Sleiman PM, Gandhi S, Jain S, Singleton A, Lees AJ, Shaw K, Bhatia KP, Bonifati V, Quinn NP, Lynch J, Healy DG, Holton JL, Revesz T, Wood NW (2005) A common LRRK2 mutation in idiopathic Parkinson's disease. Lancet 365:415–416.

Glinka Y, Gassen M, Youdim MBH (1997) Mechanism of 6-hydroxydopamine neurotoxicity. J Neural Transm Suppl:55–66.

Gu X-L, Long C-X, Sun L, Xie C, Lin X, Cai H (2010) Astrocytic expression of Parkinson's disease-related A53T α-synuclein causes neurodegeneration in mice. Mol Brain 3:12.

Haber SN (2014) The place of dopamine in the cortico-basal ganglia circuit. Neuroscience 282:248–257.

Halassa MM, Fellin T, Haydon PG (2007) The tripartite synapse: roles for gliotransmission in health and disease. Trends Mol Med 13:54–63.

Hama H, Hara C, Yamaguchi K, Miyawaki A (2004) PKC signaling mediates global enhancement of excitatory synaptogenesis in neurons triggered by local contact with astrocytes. Neuron 41:405–415.

Hirsch E, Graybiel AM, Agid YA (1988a) Melanized dopaminergic neurons are differentially susceptible to degeneration in Parkinson's disease. Nature 334:345–348.

Hirsch E, Graybiel AM, Agid YA (1988b) Melanized dopaminergic neurons are differentially susceptible to degeneration in Parkinson's disease. Nature 334:345–348.

Hoekstra JG, Cook TJ, Stewart T, Mattison H, Dreisbach MT, Hoffer ZS, Zhang J (2015) Astrocytic dynamin-like protein 1 regulates neuronal protection against excitotoxicity in Parkinson disease. Am J Pathol 185:536–549.

Hol EM, Pekny M (2015) Glial fibrillary acidic protein (GFAP) and the astrocyte intermediate filament system in diseases of the central nervous system. Curr Opin Cell Biol 32:121–130.

Irwin DJ, White MT, Toledo JB, Xie SX, Robinson JL, Van Deerlin V, Lee VM-Y, Leverenz JB, Montine TJ, Duda JE, Hurtig HI, Trojanowski JQ (2012) Neuropathologic substrates of Parkinson disease dementia. Ann Neurol 72:587–598.

Janzer RC, Raff MC (1987) Astrocytes induce blood–brain barrier properties in endothelial cells. Nature 325:253–257.

John GR, Lee SC, Brosnan CF (2003) Cytokines: Powerful Regulators of Glial Cell Activation. Neurosci 9:10–22.

Joshi AU, Minhas PS, Liddelow SA, Haileselassie B, Andreasson KI, Dorn GW, Mochly-Rosen D (2019) Fragmented mitochondria released from microglia trigger A1 astrocytic response and propagate inflammatory neurodegeneration. Nat Neurosci 22:1635–1648.

Khakh BS, Sofroniew M V (2015) Diversity of astrocyte functions and phenotypes in neural circuits. Nat Neurosci 18:942–952.

Kim C, Spencer B, Rockenstein E, Yamakado H, Mante M, Adame A, Fields JA, Masliah D, Iba M, Lee H-J, Rissman RA, Lee S-J, Masliah E (2018) Immunotherapy targeting toll-like receptor 2 alleviates neurodegeneration in models of synucleinopathy by modulating α-synuclein transmission and neuroinflammation. Mol Neurodegener 13:43.

Kim J-M, Cha S-H, Choi YR, Jou I, Joe E-H, Park SM (2016) DJ-1 deficiency impairs glutamate uptake into astrocytes via the regulation of flotillin-1 and caveolin-1 expression. Sci Rep 6:28823.

Kordower JH, Olanow CW, Dodiya HB, Chu Y, Beach TG, Adler CH, Halliday GM, Bartus RT (2013) Disease duration and the integrity of the nigrostriatal system in Parkinson's disease. Brain 136:2419–2431.

Kostuk EW, Cai J, Iacovitti L (2019) Subregional differences in astrocytes underlie selective neurodegeneration or protection in Parkinson's disease models in culture. Glia 67:glia.23627.

Kovacs GG, Breydo L, Green R, Kis V, Puska G, Lőrincz P, Perju-Dumbrava L, Giera R, Pirker W, Lutz M, Lachmann I, Budka H, Uversky VN, Molnár K, László L (2014) Intracellular processing of disease-associated α-synuclein in the human brain suggests prion-like cell-to-cell spread. Neurobiol Dis 69:76–92.

Kuter K, Olech Ł, Głowacka U (2018) Prolonged Dysfunction of Astrocytes and Activation of Microglia Accelerate Degeneration of Dopaminergic Neurons in the Rat Substantia Nigra and Block Compensation of Early Motor Dysfunction Induced by 6-OHDA. Mol Neurobiol 55:3049–3066.

Landhuis E (2018) Tapping into the brain's star power. Nature 563:141–143.

Larsen NJ, Ambrosi G, Mullett SJ, Berman SB, Hinkle DA (2011) DJ-1 knock-down impairs astrocyte mitochondrial function. Neuroscience 196:251–264.

Lee CS, Sauer H, Björklund A (1996) Dopaminergic neuronal degeneration and motor impairments following axon terminal lesion by intrastriatal 6-hydroxydopamine in the rat. Neuroscience 72:641–653.

Lee S-W, Kim WJ, Choi YK, Song HS, Son MJ, Gelman IH, Kim Y-J, Kim K-W (2003) SSeCKS regulates angiogenesis and tight junction formation in blood-brain barrier. Nat Med 9:900–906.

Lees AJ, Selikhova M, Andrade LA, Duyckaerts C (2008) The black stuff and Konstantin Nikolaevich Tretiakoff. Mov Disord 23:777–783.

Liddelow SA et al. (2017) Neurotoxic reactive astrocytes are induced by activated microglia. Nature 541:481–487.

Liddelow SA, Sofroniew M V. (2019) Astrocytes usurp neurons as a disease focus. Nat Neurosci 22:512–513.

Loria F, Vargas JY, Bousset L, Syan S, Salles A, Melki R, Zurzolo C (2017) α-Synuclein transfer between neurons and astrocytes indicates that astrocytes play a role in degradation rather than in spreading. Acta Neuropathol 134:789–808.

Lowery J, Kuczmarski ER, Herrmann H, Goldma RD (2015) Intermediate filaments play a pivotal role in regulating cell architecture and function. J Biol Chem 290:17145–17153.

Marcaggi P, Billups D, Attwell D (2003) The Role of Glial Glutamate Transporters in Maintaining the Independent Operation of Juvenile Mouse Cerebellar Parallel Fibre Synapses. J Physiol 552:89–107.

Masamoto K, Unekawa M, Watanabe T, Toriumi H, Takuwa H, Kawaguchi H, Kanno I, Matsui K, Tanaka KF, Tomita Y, Suzuki N (2015) Unveiling astrocytic control of cerebral blood flow with optogenetics. Sci Rep 5:11455.

McKeon RJ, Schreiber RC, Rudge JS, Silver J (1991) Reduction of neurite outgrowth in a model of glial scarring following CNS injury is correlated with the expression of inhibitory molecules on reactive astrocytes. J Neurosci 11:3398–3411.

Meiser J, Weindl D, Hiller K (2013) Complexity of dopamine metabolism. Cell Commun Signal 11:1–18.

Messing A, Brenner M (2020) GFAP at 50. ASN Neuro 12.

Mishra A (2017) Binaural blood flow control by astrocytes: listening to synapses and the vasculature. J Physiol 595:1885–1902.

Miyanishi K, Choudhury ME, Watanabe M, Kubo M, Nomoto M, Yano H, Tanaka J (2019) Behavioral tests predicting striatal dopamine level in a rat hemi-Parkinson's disease model. Neurochem Int 122:38–46.

Mouse Specifics Inc. (2011) Digigait Imaging System - Indicies.

Mullett SJ, Di Maio R, Greenamyre JT, Hinkle DA (2013) DJ-1 expression modulates astrocyte-mediated protection against neuronal oxidative stress. J Mol Neurosci 49:507–511.

Nagelhus EA, Mathiisen TM, Ottersen OP (2004) Aquaporin-4 in the central nervous system: Cellular and subcellular distribution and coexpression with KIR4.1. Neuroscience 129:905–913.

Nath S, Goodwin J, Engelborghs Y, Pountney DL (2011) Raised calcium promotes α-synuclein aggregate formation. Mol Cell Neurosci 46:516–526.

Neal M, Luo J, Harischandra DS, Gordon R, Sarkar S, Jin H, Anantharam V, Désaubry L, Kanthasamy A, Kanthasamy A (2018) Prokineticin-2 promotes chemotaxis and alternative A2 reactivity of astrocytes. Glia 66:2137–2157.

Nichols WC, Pankratz N, Hernandez D, Paisán-Ruíz C, Jain S, Halter CA, Michaels VE, Reed T, Rudolph A, Shults CW, Singleton A, Foroud T, Parkinson Study Group-PROGENI investigators (2005) Genetic screening for a single common LRRK2 mutation in familial

Parkinson's disease. Lancet 365:410–412.

Nishimura RN, Santos D, Fu ST, Dwyer BE (2000) Induction of cell death by L-alpha-aminoadipic acid exposure in cultured rat astrocytes: Relationship to protein synthesis. Neurotoxicology 21:313–320.

O'Neill E, Chiara Goisis R, Haverty R, Harkin A (2019) L-alpha-aminoadipic acid restricts dopaminergic neurodegeneration and motor deficits in an inflammatory model of Parkinson's disease in male rats. J Neurosci Res 97:804–816.

Parkinson J (2002) An Essay on the Shaking Palsy. J Neuropsychiatry Clin Neurosci 14:223–236.

Perea G, Araque A (2005) Properties of Synaptically Evoked Astrocyte Calcium Signal Reveal Synaptic Information Processing by Astrocytes. J Neurosci 25:2192–2203.

Perea G, Navarrete M, Araque A (2009) Tripartite synapses: astrocytes process and control synaptic information. Trends Neurosci 32:421–431.

Powell EM, Geller HM (1999) Dissection of astrocyte-mediated cues in neuronal guidance and process extension. Glia 26:73–83.

Rizzu P, Hinkle DA, Zhukareva V, Bonifati V, Severijnen L-A, Martinez D, Ravid R, Kamphorst W, Eberwine JH, Lee VM-Y, Trojanowski JQ, Heutink P (2004) DJ-1 colocalizes with tau inclusions: A link between parkinsonism and dementia. Ann Neurol 55:113–118.

Rodriguez-Pallares J, Parga JA, Muñoz A, Rey P, Guerra MJ, Labandeira-Garcia JL (2007) Mechanism of 6-hydroxydopamine neurotoxicity: The role of NADPH oxidase and microglial activation in 6-hydroxydopamine-induced degeneration of dopaminergic neurons. J Neurochem 103:145–156.

Rostami J, Holmqvist S, Lindström V, Sigvardson J, Westermark GT, Ingelsson M, Bergström J, Roybon L, Erlandsson A (2017) Human Astrocytes Transfer Aggregated Alpha-Synuclein via Tunneling Nanotubes. J Neurosci 37:11835–11853.

Sarafian TA, Littlejohn K, Yuan S, Fernandez C, Cilluffo M, Koo B-K, Whitelegge JP, Watson JB (2017) Stimulation of synaptoneurosome glutamate release by monomeric and fibrillated α-synuclein. J Neurosci Res 95:1871–1887.

Sattler R, Rothstein JD (2006) Regulation and Dysregulation of Glutamate Transporters. In: Neurotransmitter Transporters, pp 277–303. Berlin/Heidelberg: Springer-Verlag.

Schwarz Y, Zhao N, Kirchhoff F, Bruns D (2017) Astrocytes control synaptic strength by two distinct v-SNARE-dependent release pathways. Nat Neurosci 20:1529–1539.

Shih AY, Johnson DA, Wong G, Kraft AD, Jiang L, Erb H, Johnson JA, Murphy TH (2003) Coordinate regulation of glutathione biosynthesis and release by Nrf2-expressing glia potently protects neurons from oxidative stress. J Neurosci 23:3394–3406.

Shiotsuki H, Yoshimi K, Shimo Y, Funayama M, Takamatsu Y, Ikeda K, Takahashi R, Kitazawa S, Hattori N (2010) A rotarod test for evaluation of motor skill learning. J Neurosci

Methods 189:180–185.

Simard S, Coppola G, Rudyk CA, Hayley S, McQuaid RJ, Salmaso N (2018) Profiling changes in cortical astroglial cells following chronic stress. Neuropsychopharmacology 43:1961–1971.

Sofroniew M V (2009) Molecular dissection of reactive astrogliosis and glial scar formation. Trends Neurosci 32:638–647.

Sofroniew M V, Vinters H V (2010) Astrocytes: biology and pathology. Acta Neuropathol 119:7–35.

Solano RM, Casarejos MJ, Menendez-Cuervo J, Rodriguez-Navarro JA, Garcia de Yebenes J, Mena MA (2008) Glial Dysfunction in Parkin Null Mice: Effects of Aging. J Neurosci 28:598–611.

Sousa C, Golebiewska A, Poovathingal SK, Kaoma T, Pires-Afonso Y, Martina S, Coowar D, Azuaje F, Skupin A, Balling R, Biber K, Niclou SP, Michelucci A (2018) Single-cell transcriptomics reveals distinct inflammation-induced microglia signatures. EMBO Rep 19.

Spillantini MG, Crowther RA, Jakes R, Hasegawa M, Goedert M (1998) alpha-Synuclein in filamentous inclusions of Lewy bodies from Parkinson's disease and dementia with lewy bodies. Proc Natl Acad Sci U S A 95:6469–6473.

Stellwagen D, Malenka RC (2006) Synaptic scaling mediated by glial TNF-α. Nature 440:1054–1059.

Stott SRW, Barker RA (2014) Time course of dopamine neuron loss and glial response in the 6-OHDA striatal mouse model of Parkinson's disease. Eur J Neurosci 39:1042–1056.

Streifel KM, Gonzales AL, De Miranda B, Mouneimne R, Earley S, Tjalkens R (2014) Dopaminergic neurotoxicants cause biphasic inhibition of purinergic calcium signaling in astrocytes. PLoS One 9:110996.

Su RJ, Zhen JL, Wang W, Zhang JL, Zheng Y, Wang XM (2018) Time-course behavioral features are correlated with Parkinson's disease-associated pathology in a 6-hydroxydopamine hemiparkinsonian rat model. Mol Med Rep 17:3356–3363.

Su Y, Chen Z, Du H, Liu R, Wang W, Li H, Ning B (2019) Silencing miR-21 induces polarization of astrocytes to the A2 phenotype and improves the formation of synapses by targeting glypican 6 via the signal transducer and activator of transcription-3 pathway after acute ischemic spinal cord injury. FASEB J 33:10859–10871.

Surmeier DJ (2018) Determinants of dopaminergic neuron loss in Parkinson's disease. FEBS J 285:3657–3668.

Surmeier DJ, Obeso JA, Halliday GM (2017) Selective neuronal vulnerability in Parkinson disease. Nat Rev Neurosci 18:101–113.

Sveinbjornsdottir S (2016) The clinical symptoms of Parkinson's disease. J Neurochem 139:318–324.

Swanson R, Ying W, Kauppinen T (2004) Astrocyte Influences on Ischemic Neuronal Death.

Curr Mol Med 4:193–205.

Ullian EM, Sapperstein SK, Christopherson KS, Barres BA (2001) Control of Synapse Number by Glia. Science (80-) 291:657–661.

Ungerstedt U (1968) 6-hydroxy-dopamine induced degeneration of central monoamine neurons. Eur J Pharmacol 5:107–110.

Vaccarino FM, Fagel DM, Ganat Y, Maragnoli ME, Ment LR, Ohkubo Y, Schwartz ML, Silbereis J, Smith KM (2007) Astroglial Cells in Development, Regeneration, and Repair. Neurosci 13:173–185.

Voskuhl RR, Peterson RS, Song B, Ao Y, Morales LBJ, Tiwari-Woodruff S, Sofroniew M V. (2009) Reactive Astrocytes Form Scar-Like Perivascular Barriers to Leukocytes during Adaptive Immune Inflammation of the CNS. J Neurosci 29:11511–11522.

Walsh S, Finn DP, Dowd E (2011) Time-course of nigrostriatal neurodegeneration and neuroinflammation in the 6-hydroxydopamine-induced axonal and terminal lesion models of Parkinson's disease in the rat. Neuroscience 175:251–261.

Yun SP et al. (2018) Block of A1 astrocyte conversion by microglia is neuroprotective in models of Parkinson's disease. Nat Med 24:931–938.

Zador Z, Stiver S, Wang V, Manley GT (2009) Role of aquaporin-4 in cerebral edema and stroke. Handb Exp Pharmacol:159–170.

Zamanian JL, Xu L, Foo LC, Nouri N, Zhou L, Giffard RG, Barres BA (2012) Genomic Analysis of Reactive Astrogliosis. J Neurosci 32:6391–6410.

Zhan J, Yakimov V, Rühling S, Fischbach F, Nikolova E, Joost S, Kaddatz H, Greiner T, Frenz J, Holzmann C, Kipp M (2019) High Speed Ventral Plane Videography as a Convenient Tool to Quantify Motor Deficits during Pre-Clinical Experimental Autoimmune Encephalomyelitis. Cells 8.

Zhang L-N, Wang Q, Xian X-H, Qi J, Liu L-Z, Li W-B (2019) Astrocytes enhance the tolerance of rat cortical neurons to glutamate excitotoxicity. Mol Med Rep 19:1521–1528.

Zhang Y, Barres BA (2010) Astrocyte heterogeneity: an underappreciated topic in neurobiology. Curr Opin Neurobiol 20:588–594.

Zonta M, Angulo MC, Gobbo S, Rosengarten B, Hossmann K-A, Pozzan T, Carmignoto G (2003) Neuron-to-astrocyte signaling is central to the dynamic control of brain microcirculation. Nat Neurosci 6:43–50.